General Disclaimer

One or more of the Following Statements may affect this Document

- This document has been reproduced from the best copy furnished by the organizational source. It is being released in the interest of making available as much information as possible.

- This document may contain data, which exceeds the sheet parameters. It was furnished in this condition by the organizational source and is the best copy available.

- This document may contain tone-on-tone or color graphs, charts and/or pictures, which have been reproduced in black and white.

- This document is paginated as submitted by the original source.

- Portions of this document are not fully legible due to the historical nature of some of the material. However, it is the best reproduction available from the original submission.

FINAL REPORT

for NASA Contract NASR-176

DEVELOPMENT OF AN ORBITAL RECEIVER FOR LOW-FREQUENCY RADIO ENERGY FROM THE PLANET JUPITER

A. G. Smith and G. R. Lebo
Co-Principal Investigators

Department of Physics and Astronomy
University of Florida

Gainesville, Florida
February 7, 1969

TABLE OF CONTENTS

I. SUMMARY

The University of Michigan and the University of Florida are jointly proposing a series of radiofrequency experiments to be performed by the Pioneer F/G Asteroid-Jupiter spacecraft. The Michigan group has extensive experience in space radio astronomy, while the Florida scientists have been studying the low-frequency Jupiter radio emission since its discovery. Both groups have extensive facilities and personnel to devote to such a project. The proposed experiments are aimed at elucidating the positions, spectra, polarization, sizes, and motions of the powerful decametric sources on Jupiter, as well as studying the effect of the interplanetary medium (including the asteroid belt) on the radiation. The measurements will provide critical tests of theories suggesting that the Jovian radiation is confined to sharp, geometrical beams. A related experiment will use the antenna system to measure ambient plasma density in the interplanetary medium, the asteroid belt, and the Jovian magnetosphere, both as an end in itself and as an important aid in interpreting the radio data. The results are expected to contribute substantially to our understanding of the radiation mechanisms and physical environment of the largest planet in the solar system, as well as the interplanetary medium itself. As a cost-free by-product, the low-frequency solar bursts that will be recorded will provide information on the outer corona at a time of sunspot minimum. An attractive aspect of the experiment package is that while it takes full advantage of the encounter phase of the mission, it also utilizes the long cruise mode to accumulate critical data which could not be obtained from near-earth orbits; these data are of such significance as to justify the flight even if difficulties should arise before or at encounter.

II. OBJECTIVES AND MAJOR REQUIREMENTS

1. OBJECTIVES

(1). Jupiter Science

1. Decametric Radio Source Location

Is the radio source in the magnetosphere near Io, or is it in the planetary atmosphere, perhaps at the foot of the magnetic tube including Io? What is the relationship between the source and the magnetic pole? To answer these questions it will be necessary to fix the absolute positions of the sources with an accuracy of a small fraction of the size of the planetary disc. Section IV-2 describes a pulse-ranging experiment which is capable of determining source positions to an accuracy of the order ot 10^3 Km.

2. Decametric Source Size

How large is the radio source? If the radiation is beamed into space, how wide is the beam? The source size determines the beam width if the source is a group of coherently radiating electrons. Is the millisecond (S) burst source a spatial collection of the microsecond (P) pulse sources discovered by Flagg and Carr, or are the S and P sources unrelated? Does the source size change with frequency? The pulse-ranging experiment (see section IV-2) provides means by which these questions can be answered.

3. Decametric Source Motion

Does a given source move along Jupiter's magnetic field lines? If so, does it radiate while moving toward the pole or away from the pole as predicted by Ellis? The validity of Ellis' popular theory hinges on the answers to these questions. The pulse-ranging experiment (Section IV-4) will provide accurate delineation of source motions.

4. Spectrum

It is especially important to define the low-frequency tail of the spectrum, since the best ground-based data indicate that a major portion of the radiofrequency energy resides in this tail. Any attempt to establish an energy budget or to assign an energy source for the

emission process depends critically upon these measurements. It is also important to make measurements with improved sensitivity in the present gap between the decametric and microwave regions, as a means of linking these regions. Section IV-5 describes the approach to this problem.

5. Decametric Burst Characteristics

What is the true (undistorted) duration of a Jovian burst? Is the low-frequency emission quasi-continuous as certain observations now suggest? Does the L burst structure arise in the interplanetary medium as suggested by Douglas? Are the S bursts formed entirely in the Jovian environment as several lines of evidence now indicate? How does the true burst structure depend on λ_{III} and the position of Io? The burst analysis circuitry described in Section IV-6 will be used to answer these questions.

6. Decametric Polarization

Between 22 MHz and 10 MHz the decametric polarization undergoes a transformation from predominantly right-hand to a symmetrical distribution of right-hand and left-hand events. Does this trend continue, with the radiation becoming essentially all left-hand at very low-frequencies? The answer to this question has a crucial bearing on radiation mechanism theories, and it can be provided only by measurements made at short distances from the planet. Section IV-8 describes the experimental procedure to be used in making the polarization measurements.

(2). Low-Frequency Solar Burst Observations

The University of Michigan Radio Astronomy Observatory has accummulated substantial experience in the recording and interpretation of solar bursts in the extreme low-frequency regions observable only from spacecraft. While solar observations are not a prime objective of the proposed experiment, they can and will be obtained as a cost-free by-product of the Jupiter radiometer system. During the long incerval of the cruise mode it will be possible to extend present observations to a period near solar minimum, a matter of distinct astrophysical interest because of the substantial changes known to occur in the corona as the solar cycle progresses. At that stage of the cycle it will be reasonable to expect about ten strong bursts per month. The wide range of available frequencies will permit study of a very extensive region of the corona.

If another spacecraft (e.g. OGO-V or IMP-I) is operative during the Jupiter mission, simultaneous observations from both spacecraft will make it possible to specify more accurately the run of electron density in the outer corona from the geometry and time lags involved in the observations. It will also be of interest to watch for systematic changes in the burst fine structure created by the interplanetary medium as the sun-probe distance increases (this is of course the inverse of the Jupiter pulse characteristic experiment, and the two sets of observations should strongly reinforce each other).

(3). Plasma Measurements

The objective of this experiment is to determine the ambient plasma density throughout the entire trajectory of the asteroid/Jupiter probe. The method will be that of monitoring the impedance of the spacecraft antenna system at several radiofrequencies selected to conform to the expected plasma densities. During the cruise mode information will be obtained on the density of the interplanetary medium out to a solar distance of 5 A. U. Information will also be obtained on irregularities in the interplanetary medium, and it may be possible to say whether the regular spiral structure of plasma streams is maintained to 5 A. U. or if, as has been suggested, the streams break up into turbulence inside Jupiter's orbit. The antenna impedance measurements will be of further importance in maintaining a continuous check on the overall system gain in the determination of absolute radio flux levels -- that is, in establishing the shape of the low-frequency tail of Jupiter's decametric spectrum.

It will be of considerable interest to determine if discontinuities are observed in the asteroid belt, either as the result of entrainment of plasma or the generation of plasma in the wakes of the asteroids themselves.

During the encounter phase of the mission, measurements will be obtained of the plasma densities in the Jovian magnetosphere. Experience gained by the Michigan group from rockets and earth-orbit experiments has demonstrated the importance of such measurements in interpreting radiofrequency noise observations made in a plasma environment. The plasma measurements, for example, make it possible to distinguish trapped radio noise from that capable of escaping to the external world. Since Michigan astronomers have identified localized trapped noise in

the terrestrial magnetosphere, it doubtless exists in the Jovian magnetosphere and should not be confused with the escaping signals observed at the earth. The plasma measurements thus provide important back-up for the radiofrequency measurements to be made during the mission.

2. MAJOR REQUIREMENTS

(1). RFI

The fact that this experiment is necessarily designed to monitor weak radio signals makes it vulnerable to spurious radio noise generated by the spacecraft itself. Several University of Michigan orbital radiometer experiments have been severely limited or completely negated by interfering radio signals generated by switches, clocks, inverters, etc. related to other experiments or to spacecraft housekeeping. Recently launched satellites have demonstrated that if adequate care is taken in all phases of design and fabrication, radio interference can be virtually eliminated. In view of the unique importance of radio observations in the case of Jupiter, it is impossible to overemphasize the requirement that the spacecraft be substantially radio quiet.

(2). Experiment Support -- Ground Observations

The decametric radio source positions can be calculated if the time of arrival of a microsecond (P) pulse or S burst is known at the spacecraft and at the earth. Therefore, it is essential that at least one ground radio observatory operate as an integral part of the experiment. The University of Florida's two present observatories (one near Huanta, Chile, the other in Dixie County, Florida) require only modest additions to their equipment to perform these ground-based observations. Since both observatories are at about the same longitude, Jupiter will be visible a maximum of about twelve hours per day from the ground. The data available for pulse ranging could be doubled if a small field station were established in Australia or New Zealand. Examples of suitable locations for such a field station are the Mount John Observatory in New Zealand, with which the University of Florida is officially associated, or the NASA tracking station at Carnarvon in western Australia. The latter would provide somewhat more complete

coverage as it is located 175 degrees in longitude from the Huanta Observatory, whereas the New Zealand longitude difference is about 120°. Since the field station would be used primarily in connection with the pulse-ranging experiment, it would be considerably less complex than the existing ground observatories, which will provide general ground based back-up for all phases of the experiment.

(3). Experiment Support -- Other Experiments

While the Michigan/Florida experiments are not critically dependent on other on-board experiments, the data derived from certain such experiments would improve the accuracy and enlarge the interpretive possibilities of the radiometer and antenna impedance results. The contributing experiments that might logically be expected to be aboard are as follows:

1. Magnetometer Experiment

Any theory of the mechanism responsible for Jupiter's radio emission will necessarily rely heavily on the magnetic field strength (B) and direction. Ground-based microwave measurements have produced brightness temperature maps of Jupiter and its surroundings. These maps, interpreted in terms of a synchrotron model, can be transformed into maps of BE^2 where E is the electron energy (see section III). With these maps, and with B determined by an on-board magnetometer, the electron energy (E) can be calculated and compared with the value calculated from the beaming and source-size experiments described in section IV-2. It is also necessary to know the vector magnetic field in order to transform the antenna impedance measurements into electron plasma densities, an interpretation that will greatly increase the value of the observations.

2. Radio Propogation Experiment

One of the uncertainties in the pulse-ranging experiment is the propagation velocity (V) of 20.75 MHz radio waves. Since V depends directly on $\int n_e \, dr$, this uncertainty can be reduced practically to zero if the integrated number of interplanetary and ionospheric electrons between the spacecraft and the earth is known from a radio propogation experiment.

It has also been proposed by Douglas and Smith of Yale that the decametric L bursts are scintillations produced by interplanetary electrons, the original Jovian radiation being envisaged as being continuous or quasi-continuous. While a systematic change in burst

character with Jupiter-spacecraft distance will provide a critical test of this important hypothesis, the experiment can be made more quantitative by comparing $\int n_e$ dr from the propagation experiment with the numerical L-burst "scintillation" (i.e., modulation) index.

3. Electron Probe Measurements

The antenna impedance experiment provides a means of calculating electron density in the vicinity of the spacecraft. Because sampling is in effect done over a large volume, such an experiment is less susceptible than is a local probe to systemmatic errors introduced by the spacecraft geometry. However, an on-board electron probe would provide valuable comparison data for the antenna impedance experiment. Such data would also provide an alternative to the radio propagation experiment in evaluating $\int n_e$ dr for the scintillation studies discussed in the preceding section.

(4). Spacecraft Position and Timing Accuracy

The time of arrival of a pulse at the spacecraft is one of the parameters being measured in the pulse ranging experiment. It is imperative that this parameter be measured to an accuracy of 0.1 msec in the earth frame. This accuracy can be obtained by phase-locking the spacecraft clock to a ground-based atomic standard or by frequently updating a good (1 part in 10^8) spacecraft clock. It is beyond the state of the art to construct spacecraft time standards capable of retaining absolute time to an accuracy of 10^{-4} sec over a period of two years.

Another parameter that must be measured accurately is the earth-spacecraft distance. The pulse ranging experiment is geometrical in nature, with the earth-spacecraft distance being one leg of a triangle. Since the position of the radio source can be determined to no greater accuracy than that to which the spacecraft position is known, an accurate spacecraft ranging system will be very useful for this experiment.

III. BACKGROUND AND JUSTIFICATION

Thirteen years have elapsed since Burke and Franklin discovered that Jupiter is a source of intense radio outbursts at decametric wavelengths. During this interval it has become evident that Jupiter is one of the most spectacular and puzzling radio sources in the sky. It is also evident that Jupiter is unique among the planets of the solar system in this respect. The radio observations have added extensively to our knowledge of the physical conditions of the planet and its environment, and this information has a particularly strong bearing on space missions involving Jupiter. The peculiar nature of the Jovian radio spectrum raises important questions which can be answered only by conducting experiments from spacecraft, both in earth orbit and in the vicinity of the planet itself.

1. The Jovian Radio Spectrum

Figure 1 is an overview of the Jovian radio spectrum, including both the decametric and microwave regions. By far the most striking feature is the strong, nonthermal peak in the decametric region. At wavelengths below about 3 cm the microwave spectrum is essentially thermal, but in the decimetric region it, too, becomes strongly nonthermal. Between the decametric and decimetric regions there is an extensive gap in which radiation has yet to be detected (dashed lines).

Toward the lowest ground-based frequencies the flux increases rapidly both in intensity and in frequency of occurrence (Fig. 2ab). Figure 2c shows that the time-averaged flux increases as rapidly as the 8th power of the wavelength in the middle decametric region. Just as the decametric flux tends to dominate the entire spectrum, so does the low-frequency tail dominate the decametric region itself. Clearly, any meaningful evaluation of the radiofrequency energy balance depends critically upon the use of space measurements to extend this high-energy tail to frequencies well below the ionospheric cut-off near 5 MHz. While useful measurements can be made from earth orbit, an unparalleled opportunity to complete the spectrum is provided by a Jupiter fly-by. The two major sources of interference are the sun and the earth. Solar burst interference, which is prominent at these frequencies, will be

Fig. III-1. Radio-Frequency Spectrum of Jupiter.

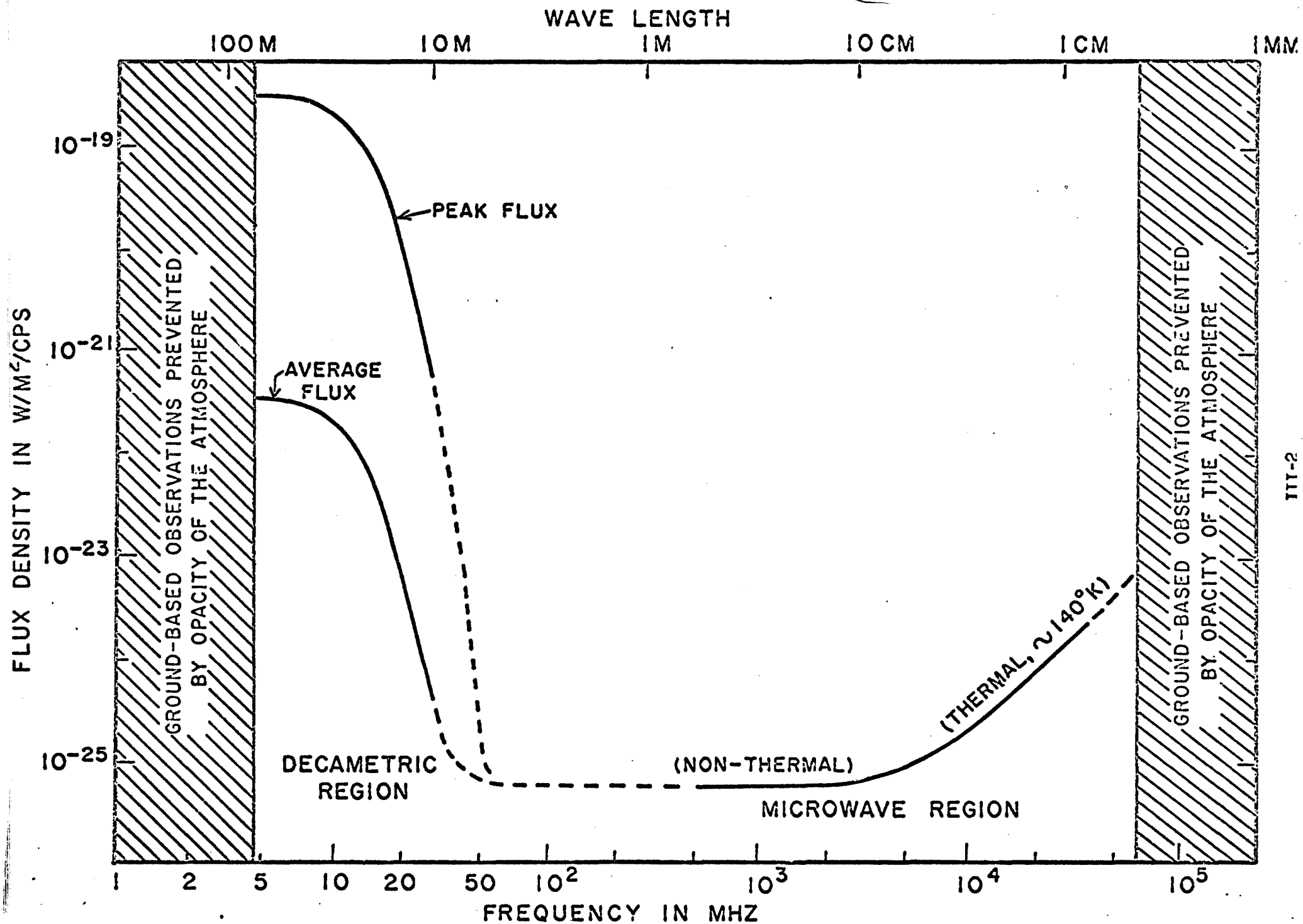

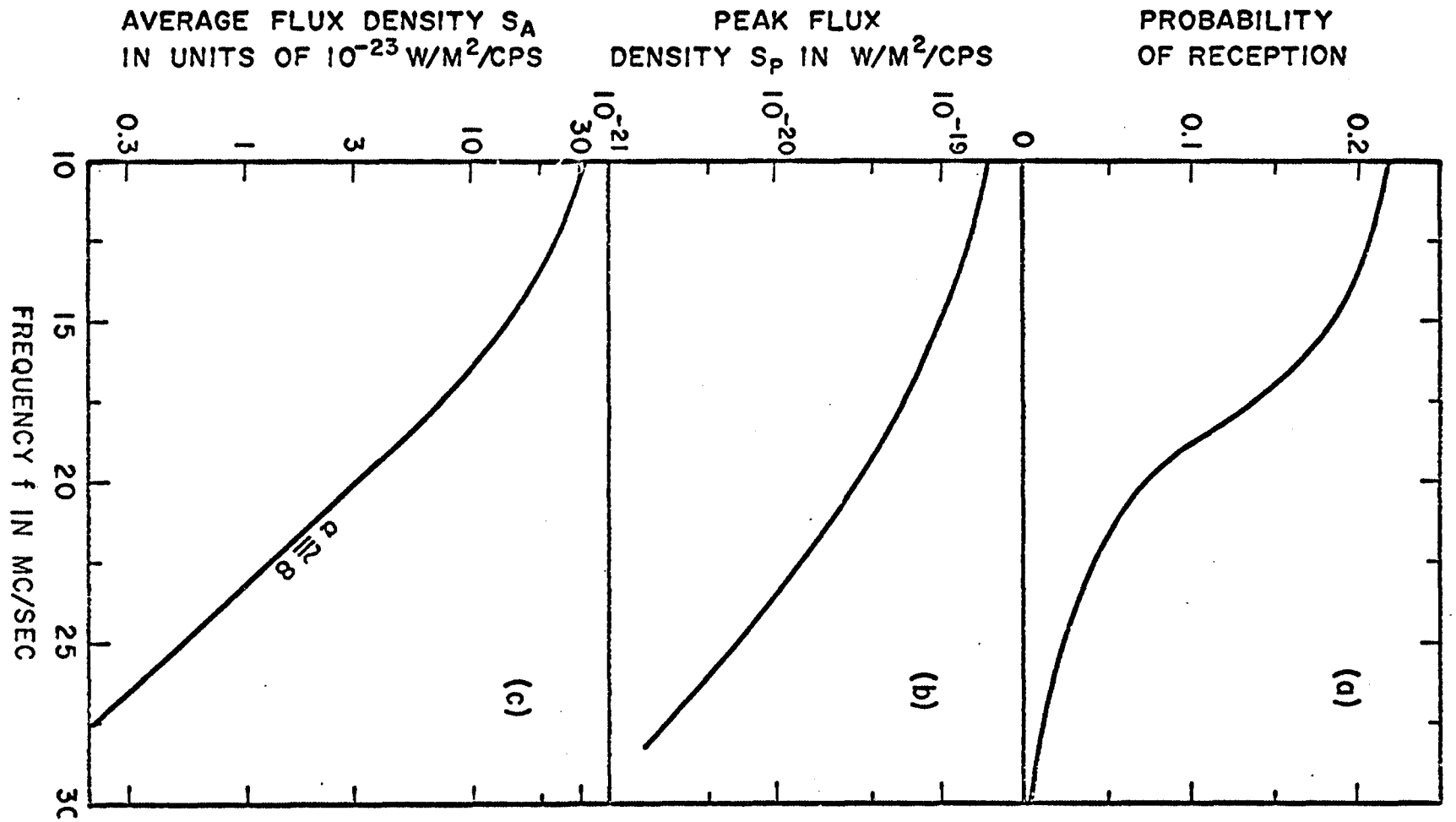

Fig. III-2. (a) Probability of reception of Jovian radiation as a function of observing frequency. (b) Peak flux density of Jovian radiation as a function of frequency. The points are averages of the five strongest bursts received at each frequency during an apparition. (c) Time-averaged flux density of Jovian radiation as a function of frequency. University of Florida data.

reduced by a factor of 25 during the mission, while the reduction in terrestrial noise will approach infinity. Near encounter it should readily be possible to detect Jovian flux in the gap between the decametric and microwave regions, something that has thus far defied efforts with large ground-based instruments.

2. Jovian Radio Sources

Although the decametric emission is intermittent in its occurrence, statistical analyses reveal several interesting periodicities. First, reception of the radiation is strongly correlated with the rotation of the planet. Figure 3 shows the probability of receiving emission at a number of frequencies as a function of the longitude of Jupiter's central meridian. It is evident that radiation is received far more often when certain critical longitudes are turned toward the earth, a phenomenon that has led rather naturally to terming these regions "sources". It can be seen from the figure that there are three prominent sources, A, B, and C, although B at times appears to be double. It is also evident that the sources are directional in character, for their angular widths are far less than 180° of longitude.

The foregoing method of analysis defines the Jovian longitudes of the sources, but it reveals nothing about their latitudes or their altitudes above the surface of the planet. Information on the sizes of the sources has been derived from the technique of "very long baseline interferometry" introduced by T. D. Carr of the Florida group in 1964. In this method, independent tape recordings are made of the signals at widely separated sites, and these records are later played back together into a correlator to produce interferometric fringes, the visibility of which is related to source size. Using baselines of 56, 210, 880, and 7040 km, the Florida group has thus far established an upper limit of 1" of arc for the apparent source size, indicating that the source diameters are less than 2% of that of the planet itself.

It is evident from Figure 3 that at best emission is received only 50% of the time even when the principal source, "A", is on the central meridian. The innermost Galilean satellite, Io, acts as a switch to control the radiation, with the favorable configurations occurring when Io is 90° or 240° from superior conjunction with Jupiter. The result is a double periodicity, involving both the rotation of the

planet and the orbital motion of its satellite, so that the locations of the sources are best displayed on a 2-dimensional plane, as in Figure 4. Possible influences of the remaining major satellites are moot, but certainly much weaker than the Io effect; it is quite possibly significant that of the four major satellites, Io alone probably orbits within Jupiter's magnetosphere.

The prominence of the Io effect inevitably raises a question as to whether the actual emission source is more closely associated with the satellite than it is with the planet itself, a question that has not been answered by the techniques used to date. While present techniques of long baseline interferometry provide information on source size, they do not define absolute source position. It is in fact unlikely that the phase coherence essential for highly precise position measurements can be maintained in decametric experiments conducted beneath the terrestrial ionosphere. The present proposal outlines a simple pulse-ranging experiment that is capable of providing Jovian source locations with a precision that will readily distinguish between competing theories of the emission mechanism. To achieve similar accuracy with ordinary long baseline interferometry would in fact involve baselines several times the diameter of the earth, a requirement that is of course completely impracticable.

Another factor that should not be overlooked is the advantage of making continuous measurements uninhibited by earth occultations or the intrusion of the sun. In searching for weak periodicities, such as effects from satellites other than Io, it is extremely helpful to avoid the introduction of diurnal or other artifact periodicities which confuse the data. Even with observatories widely spaced in terrestrial longitude it is impossible to avoid cyclic effects due to the changing planetary altitude, diurnal variations in the ionosphere, and so on.

3. Radiation Beaming

Several lines of evidence suggest that the radio emission from Jupiter may be emitted in rather flat sheets or beams. First, the microwave radiation shows a periodic modulation in both intensity and plane of polarization (Figure 5). This modulation is adequately explained by assuming that Jupiter's magnetic axis is (like that of the earth) inclined about 10° to the axis of rotation, while the

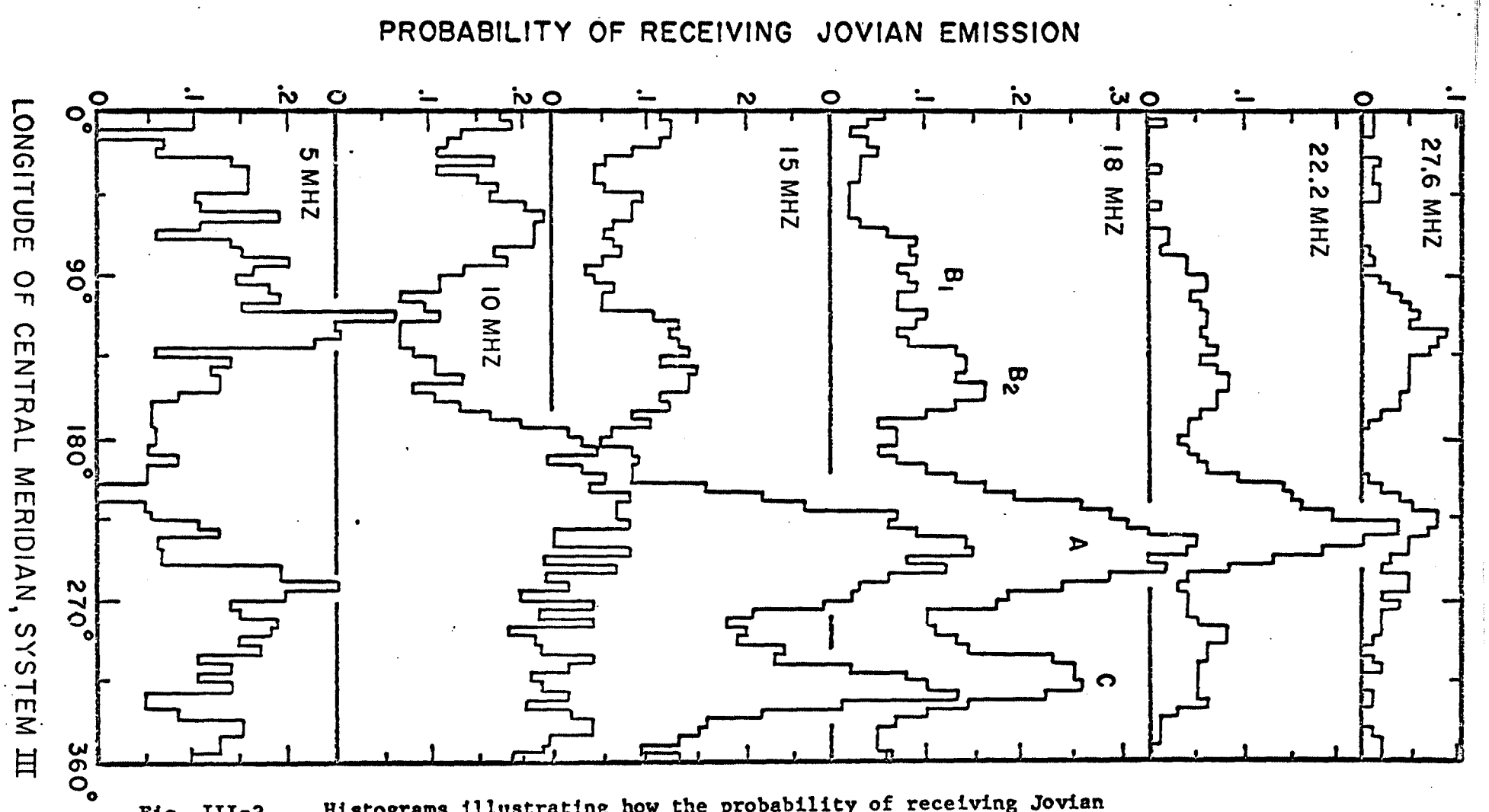

Fig. III-3. Histograms illustrating how the probability of receiving Jovian radiation varies with the longitude of the central meridian. The probability of reception for a given 5° longitude zone is the fraction of observing time during which signals were detected when that zone was on the central meridian. The data are combined observations of the University of Florida Radio Observatory and the Maipu Radioastronomical Observatory of the University of Chile for the apparitions of 1961 and 1962. (An "apparition" is the interval between successive conjunctions of the planet with the sun, or about 13 months.)

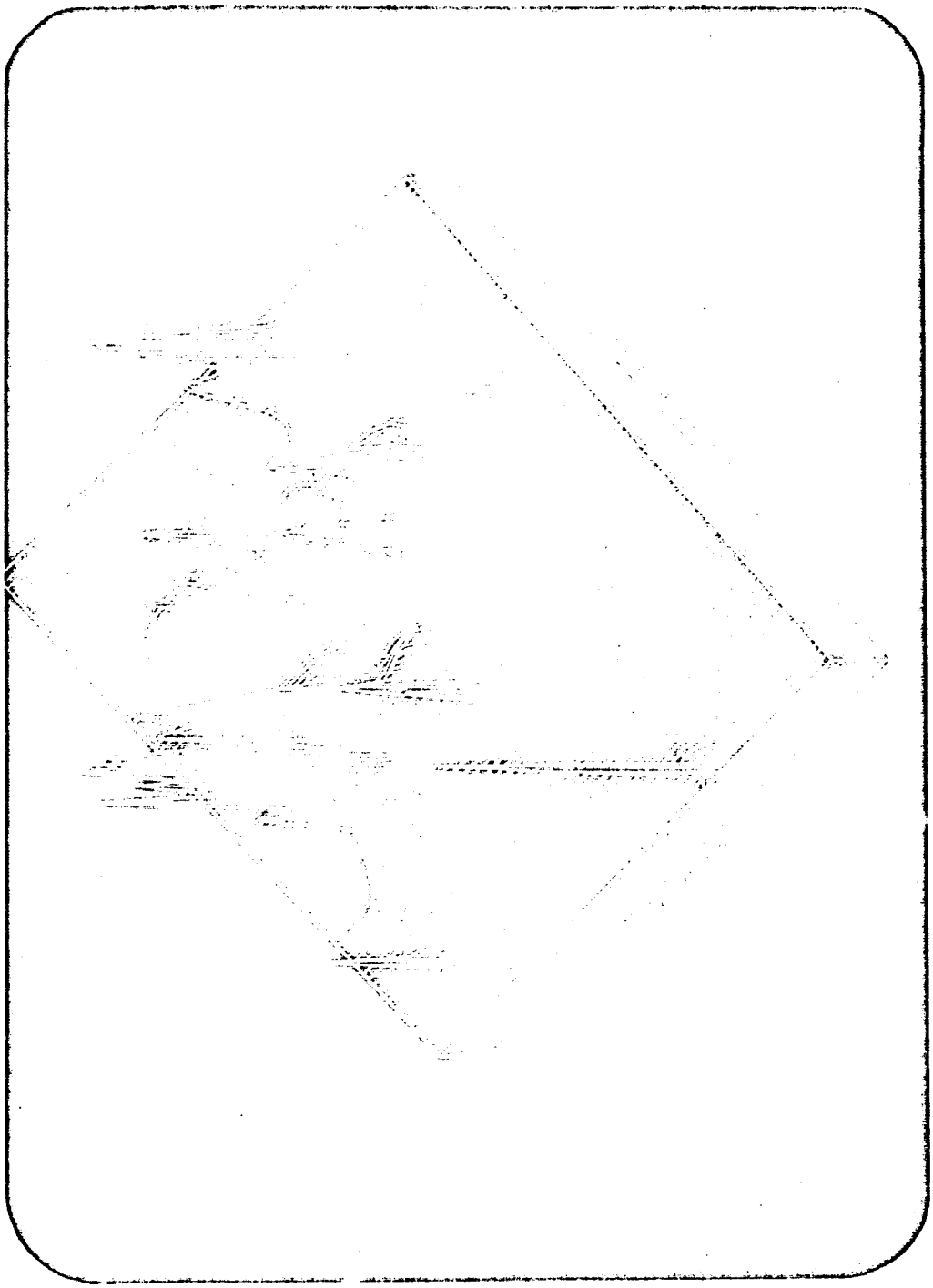

Fig. 4. 3-dimensional plot illustrating the simultaneous influence on Jupiter's decametric emission of the orbital position of Io and the Jovian longitude facing the earth. The vertical coordinate depicts the relative Jovian flux received at the earth.

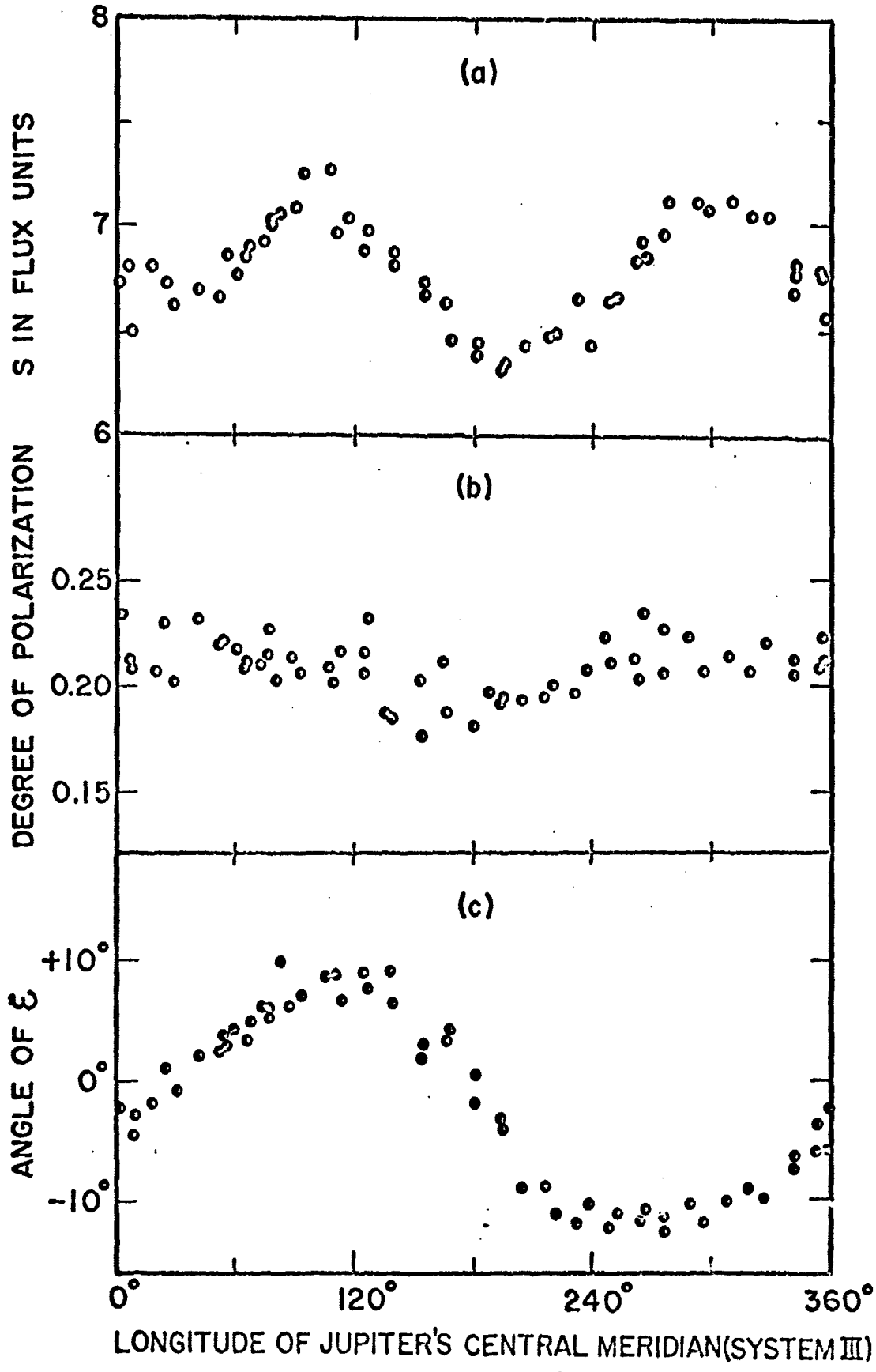

Fig. III-5. Changes in the Jovian microwave flux with rotation of the planet. The angle in (c) is the angle between the electric vector and the plane of Jupiter's equator. Adapted from J. A. Roberts and M. M. Komesaroff.

microwave flux is emitted in a thin biconical sheet as a result of synchrotron radiation from relativistic electrons near the magnetic equator (Figure 6). The resultant wobbling of the radiation sheet will cause it to sweep up and down across the earth as Jupiter rotates, producing the observed intensity modulation.

A far larger modulation component is observed in the decametric radiation. Figure 7 suggests that this modulation has a periodicity close to that of Jupiter's 12-year orbital motion about the sun. Again the effect can be explained if the radiation is emitted in a conical sheet which is inclined to the ecliptic because of the tilt of Jupiter's axis. A related observation is that the rotational period of the radio sources appears to undergo a cyclic variation whose period is again close to 12 years (Figure 8). Gulkis and Carr of the Florida group have pointed to the fact that this effect might be expected if the radiation took the form of a sheet whose intersection with the ecliptic is precessing with the 12-year orbital period.

The foregoing beaming hypotheses represent important theoretical advances which explain certain puzzling observational phenomena. However, they are not the only conceivable hypotheses; Jupiter's orbital period, for example, is close to that of the sunspot cycle, and thus the phenomena might be solar rather than geometrical in origin. Direct confirmation of beaming can be achieved by making simultaneous observations from widely separated points in space, e.g., from the earth and from the proposed Jupiter/asteroid probe (the baseline provided by an earth orbit would be totally inadequate). The cruise mode of the fly-by mission affords an unparalleled opportunity to map the intercepts of the hypothetical beams with the orbital plane, while the expected deviation from this plane at encounter will provide a scan in the perpendicular direction. Once more, simple measurements will provide critical tests of the competing theoretical models of the planet.

4. Detailed Nature of the Radiation

Except for the rotational modulation referred to in the preceding section, the microwave emission is quite stable. The brightness distribution (Figure 9) is entirely consistent with the assumption that it is synchrotron radiation from relativistic electrons trapped in a Jovian radiation belt.

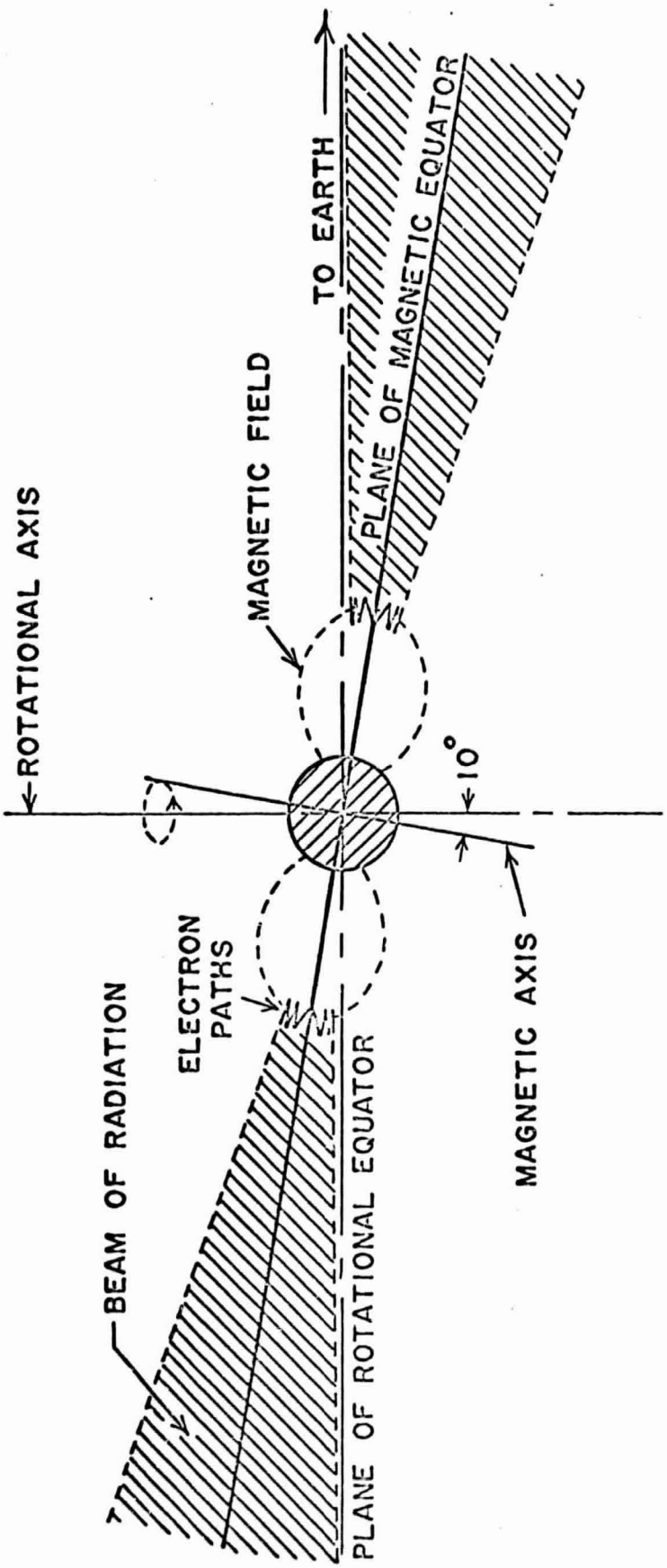

Fig. III-6. Beaming of Jovian Microwave radiation in a biconical sheet (shaded regions).

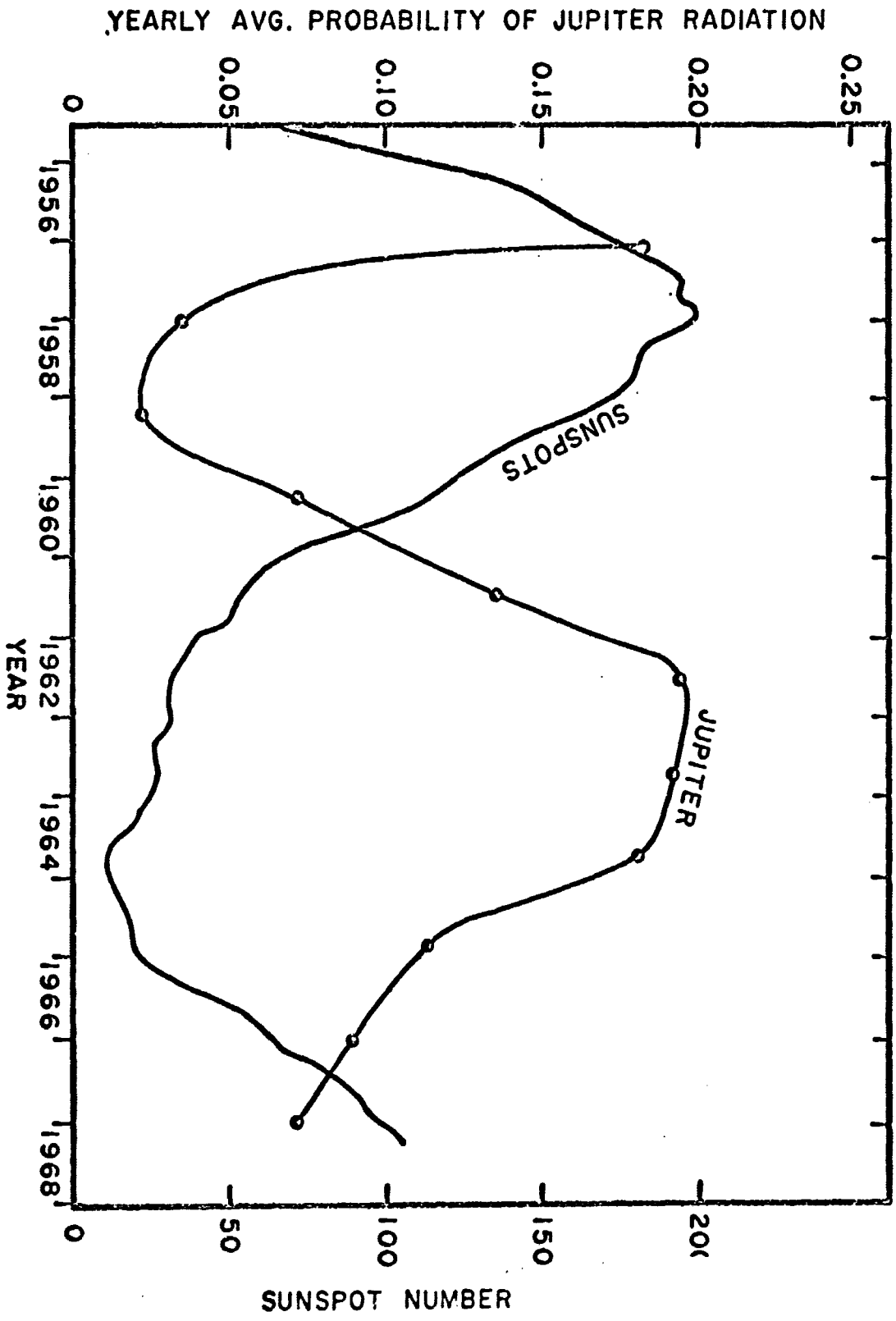

Fig. III-7. Long-term variation in the probability of receiving 18-Mc/sec flux from Jupiter. Each point is the average over all longitudes for an entire apparition. University of Florida Radio Observatory.

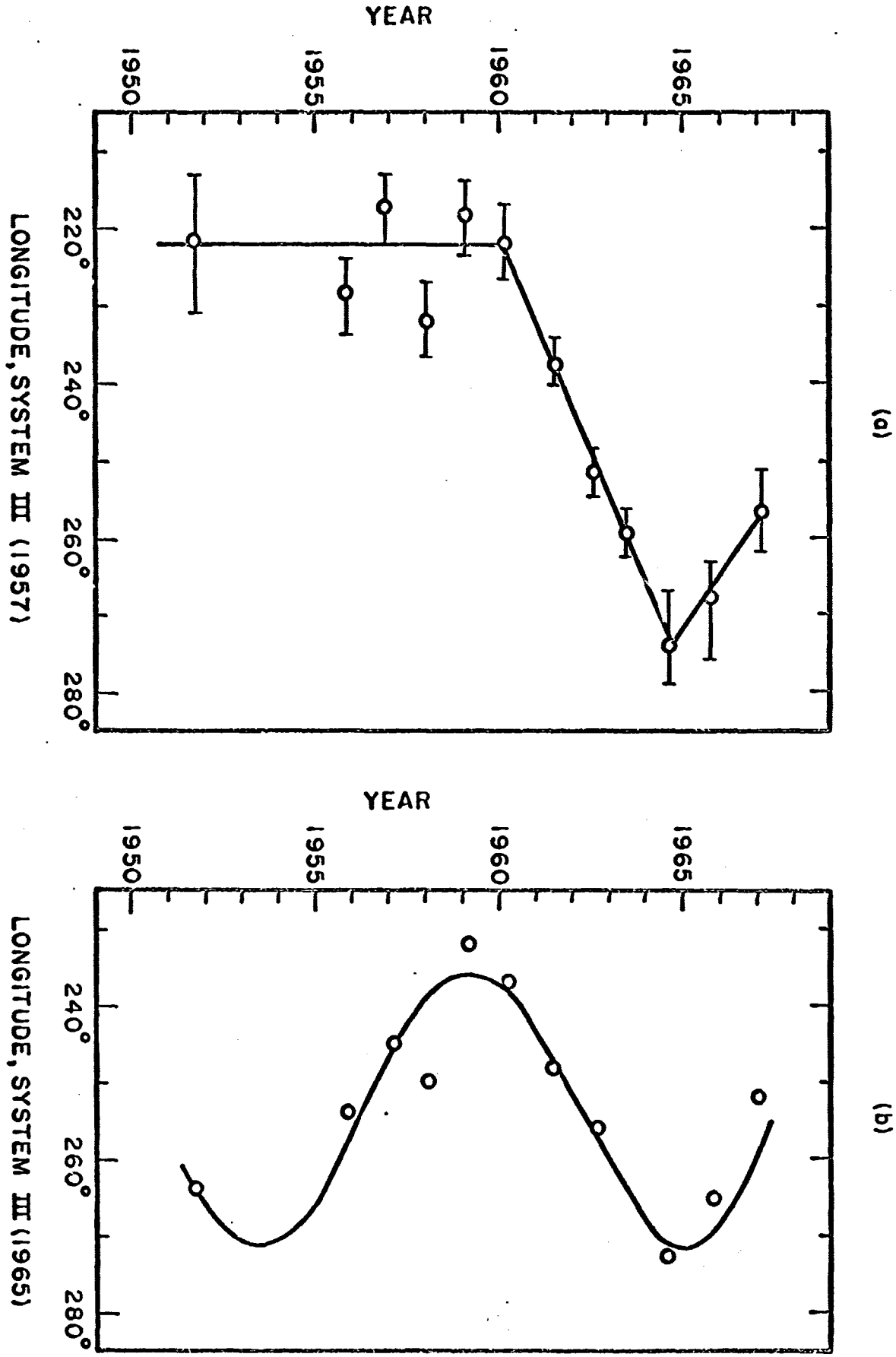

Fig. III-8. "Drift" of Jupiter's principal decametric source A in different longitude systems. (a) Drift in the "official" System III, whose rotational period is defined as $9^h\ 55^m\ 29^s.37$. (b) Drift in a special longitude system with a period of $9^h\ 55^m\ 29^s.67$.

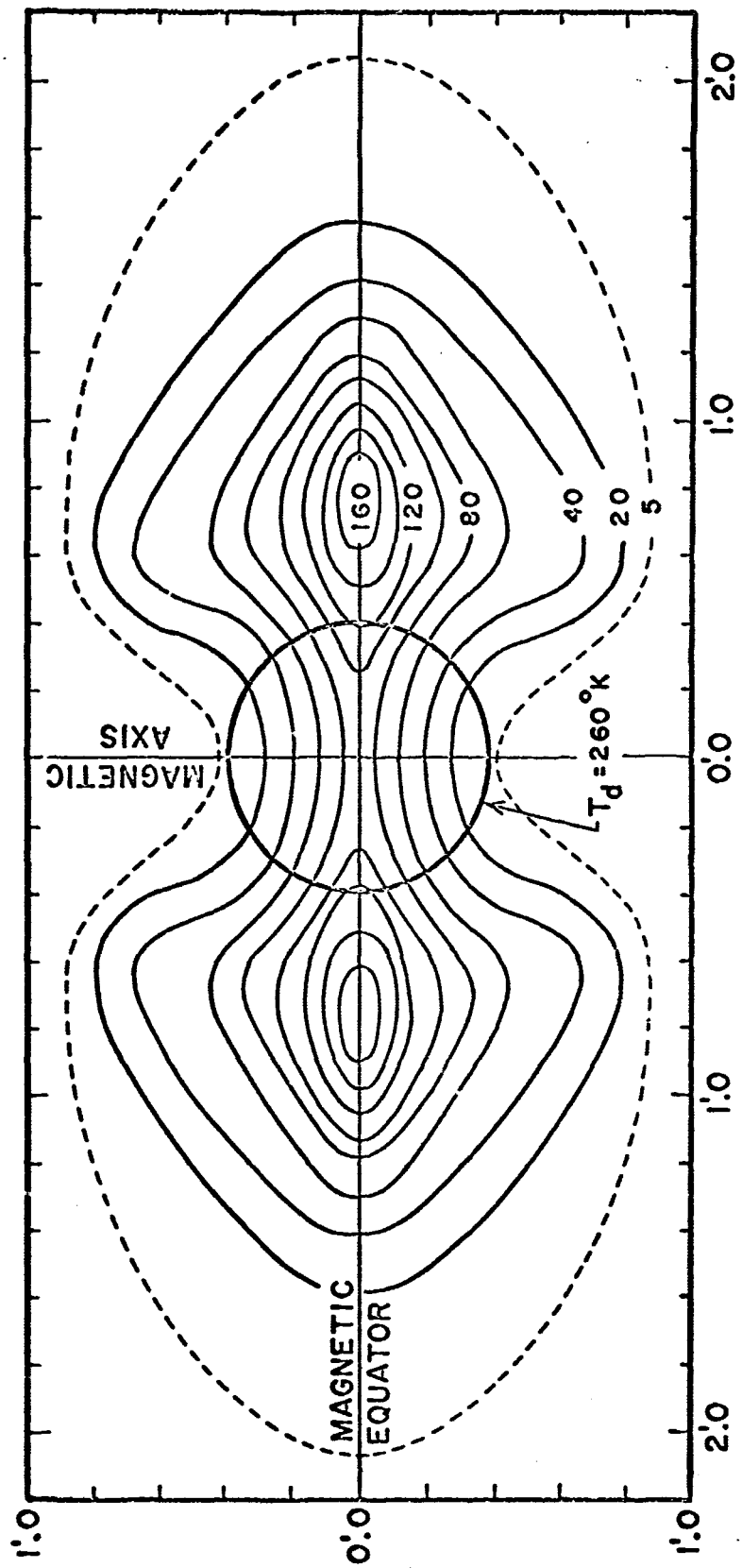

Fig. III-9. The Jovian radiation belts as outlined by 10.4-cm radio observations. The contours show the brightness temperature T_b in °K. The scale of the map is shown in minutes of arc for Jupiter at the standard distance of 4.04 AU. After Berge.

The decametric radiation, on the other hand, is highly sporadic and bursty (Figure 10). Most often the bursts are composed of pulses having durations ranging from a few tenths of a second to several seconds. Not only does the terrestrial ionosphere cause scintillation of these bursts (Figure 11), but J. N. Douglass and H. J. Smith (formerly of Yale) have shown that the bursts themselves may represent a modulation imposed by the interplanetary medium.

A somewhat less common component of the radiation consists of very short, sharp bursts lasting only a few milliseconds, or even tens of microseconds. As Figure 12 indicates, many of these bursts have rise times shorter than 10 microseconds. The work of a number of individuals at the University of Florida has shown that these bursts, at least, arise in the Jovian environment, rather than in the interplanetary medium; their occurrence is, for example, strongly correlated with the presence of source B or source C on the central meridian. Later in the present proposal it will be shown that the millisecond and microsecond pulses offer the possibility of a simple pulse ranging experiment that can be highly effective in determining the precise locations of the decametric sources. Equally interesting is the opportunity afforded by the fly-by to study the characteristics of the longer bursts as a function of the length of the optical path between Jupiter and the spacecraft. If the bursts are indeed formed in the interplanetary medium, one should observe a systematic decrease in the modulation index as the path shortens throughout the mission. Once again a simple but critical test is provided for an important hypothesis.

The decametric bursts generally display elliptical polarization. As Figure 13 indicates, the polarization is predominantly right-hand at the higher frequencies, but it becomes increasingly left-hand as the frequency decreases, reaching a symmetrical distribution at 10 MHz. Quite often, adjacent bursts in the same noise storm show opposite polarizations. This behavior is consistent with the hypothesis that the emission is cyclotron radiation from electrons orbiting in a dipolar magnetic field, the varying axial ratio reflecting the changing inclination of the magnetic pole with respect to the earth. It is of obvious interest to explore the polarization phenomena at still lower frequencies. Does the radiation there become exclusively left-hand, for example? Observations at the lowest frequencies can be made

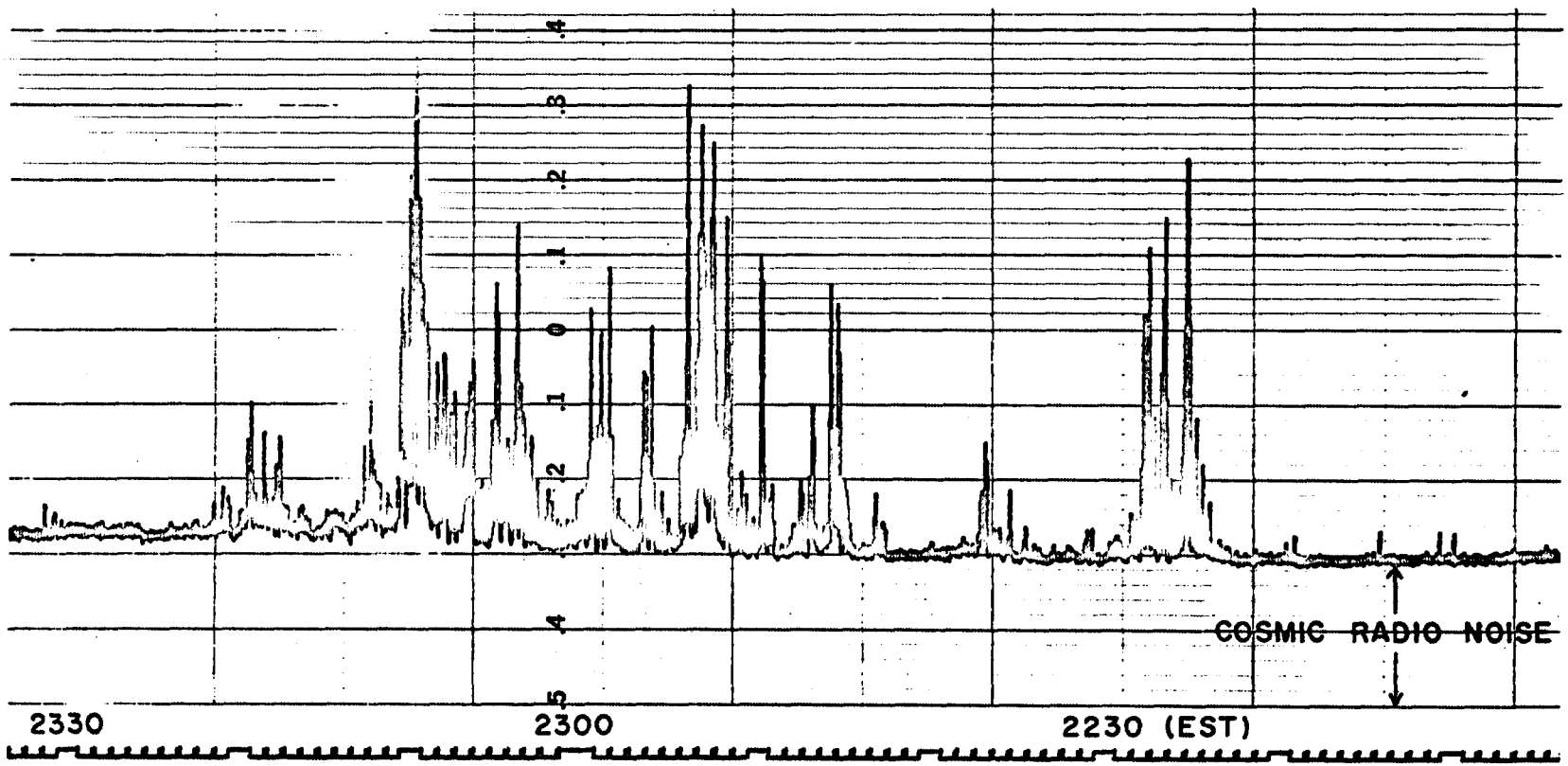

Fig. 10. A Jovian noise storm recorded at a frequency of 18 Mc/sec on January 17, 1966. University of Florida Radio Observatory.

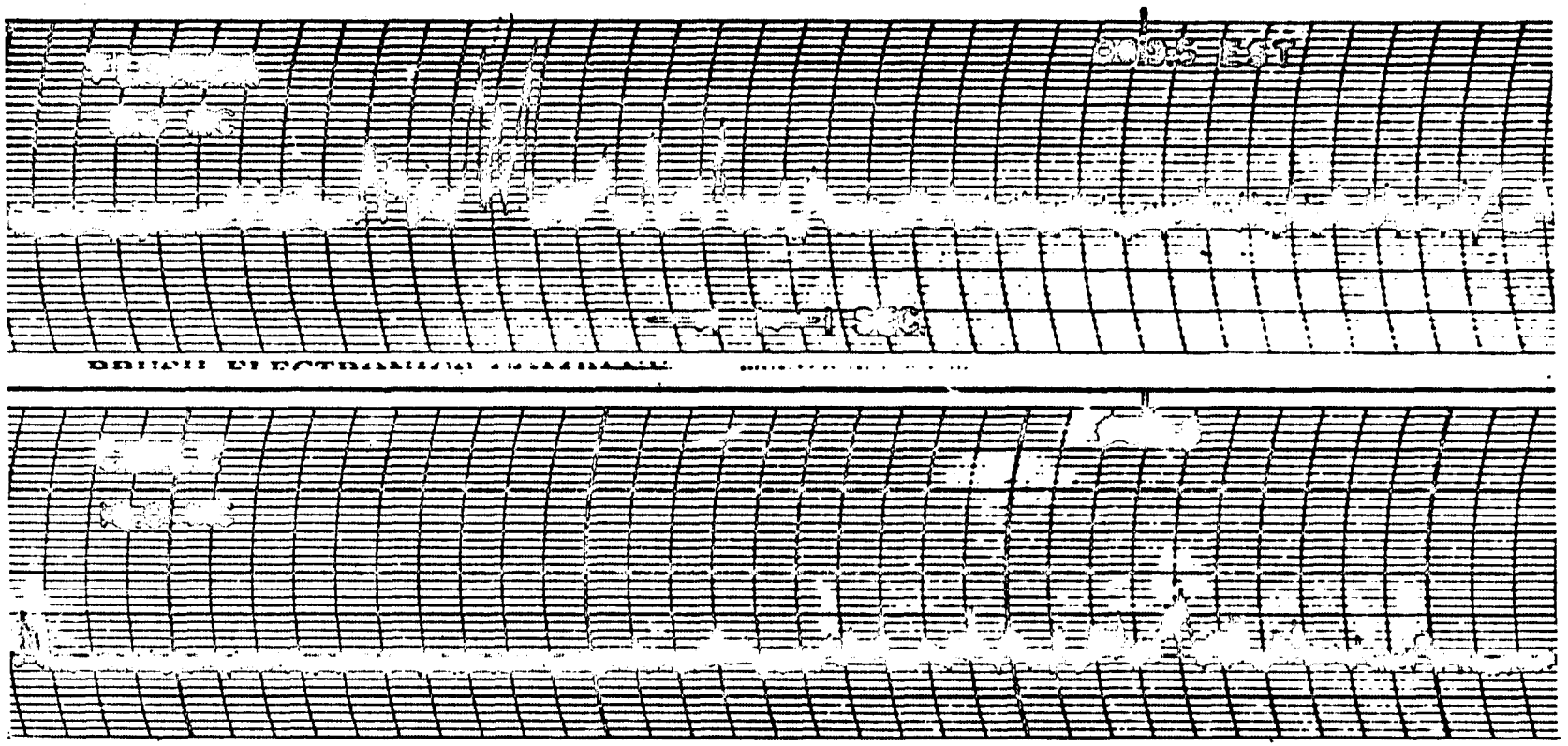

Fig. 11. High-speed records of Jovian bursts recorded simultaneously in Florida and Chile, at sites 7040 km apart. Scintillation effects appear to have produced an out-of-phase fading at the two locations. University of Florida Radio Observatory and Maipu Radioastronomical Observatory of the University of Chile.

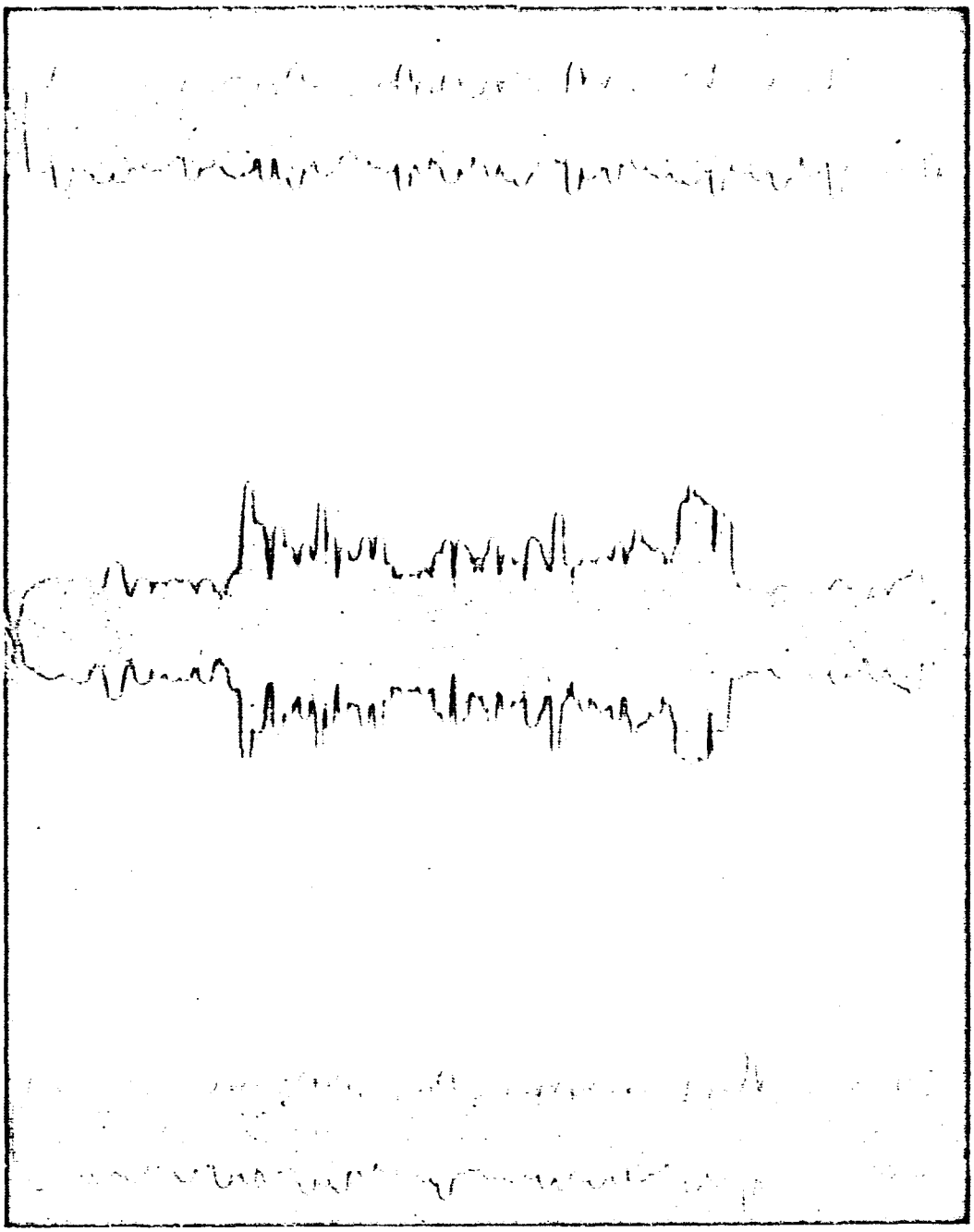

Fig. 12. Photo of msec pulse.
Sweep duration is 2000 msec.

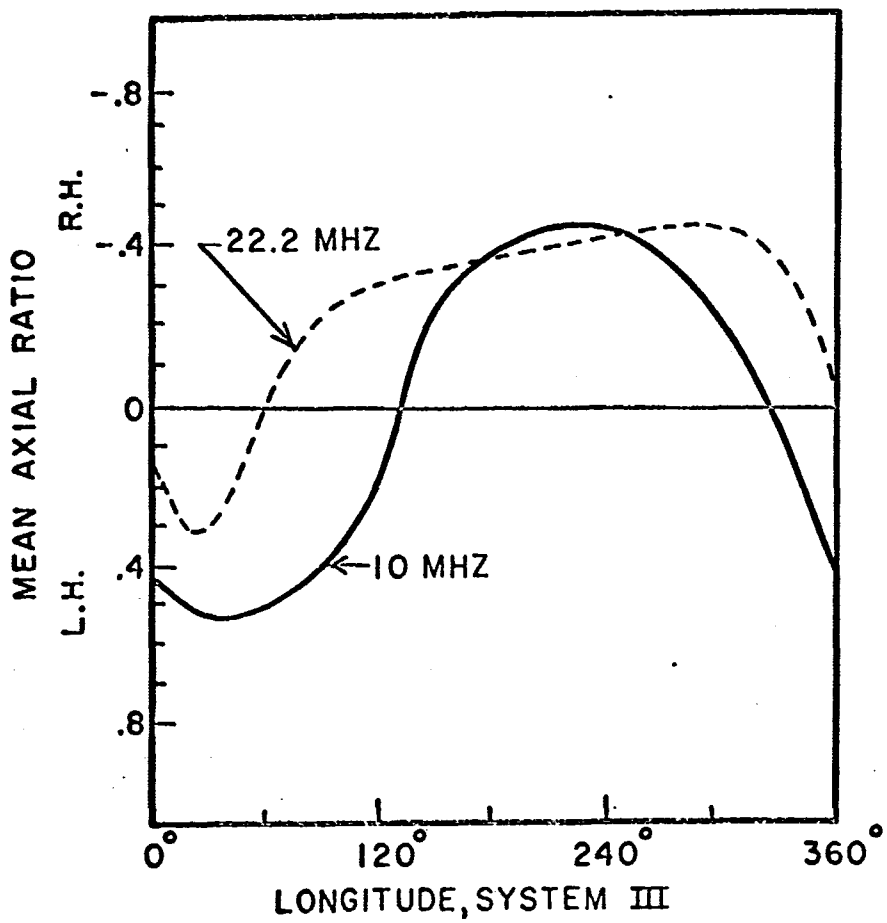

Fig. III-13. Variation with longitude of the polarization of Jovian decametric radiation. Negative values of the axial ratio represent right-hand polarization, while positive values denote left-hand polarization. Adapted from T. D. Carr, S. Gulkis, A. G. Smith, J. May, G. R. Lebo, D. Kennedy, and H. Bollhagen, Radio Science 69D, 1530-1536 (1965).

only in the vicinity of the planet, since differential Faraday rotation makes earth-based or earth-orbit observations impossible.

5. Outstanding Problems

It will be evident from the preceding discussion that a number of important observational problems remain to be solved before a definitive explanation of Jovian radiofrequency phenomena can be given. Solution of these problems is essential to a complete understanding of Jupiter's magnetic field, magnetosphere, and upper atmosphere; it is also essential to an understanding of the charged particle environment and energy budget of the largest planet in the solar system. Additional interest is lent by recent infrared observations suggesting that the thermal outflow from Jupiter is several times larger than the solar insolation (in the case of the earth, the thermal efflux is some 30,000 times smaller than the solar input). One is now obliged to reconsider the possibility of a "hot" Jupiter, a return to the 19th-century ideas that had been rather completely discarded, and to recognize the possibility that it is this factor which gives the planet its completely unique status as a radio source.

The following is a listing of the most significant radiofrequency problems which remain to be solved, more or less in order of their importance with regard to an understanding of the planet and its environment:

1) Location of the Decametric Sources. Is the radio source in the magnetosphere near Io, or is it in the planetary atmosphere, perhaps at the foot of the magnetic tube including Io? What is the relationship between the source and the magnetic pole? To answer these questions it will be necessary to fix the absolute positions of the sources with an accuracy of a small fraction of the size of the planetary disc.

2) Completion of the Radio Spectrum. It is especially important to define the low-frequency tail of the spectrum, since the best ground-based data indicate that a major portion of the radiofrequency energy resides in this tail. Any attempt to establish an energy budget or to assign an energy source for the emission process depends critically upon these measurements. It is also important to make measurements with improved sensitivity in the present gap between the decametric and microwave regions, as a means of linking these regions.

3) Particle and Field Measurements. Interpreted in terms of a synchrotron model, ground-based microwave interferometric studies such as Figure 9 can be transformed into maps of BE^2, where B is the magnetic field strength and E is the electron energy. To evaluate the two parameters separately, it is necessary to make independent measurements of one or the other. Thus it is of considerable importance to measure either B or E in the space surrounding Jupiter. If both are measured, a redundancy is provided which makes possible a more critical evaluation of the theories. While not part of the present proposal, it is assumed that such measurements will be an important part of the fly-by mission and that they will assist in the interpretation of the radio observations.

4) Effects of the Interplanetary Medium. Present data suggest that the long-duration decametric pulses may be formed in interplanetary space, whereas the millisecond pulses originate at Jupiter. It is clearly of great interest to obtain direct confirmation of these hypotheses by measurements made at varying distances from the planet. Additionally, it is likely that such measurements would provide important data on the solar wind itself.

5) RF Beaming. Hypotheses based on several kinds of observational evidence suggest that Jovian radiofrequency emission is emitted in relatively thin beams. The reality of these hypotheses should be established by correlating observations made simultaneously from widely separated points in space.

6) Low-Frequency Polarization. Between 22 MHz and 10 MHz the decametric polarization undergoes a transformation from predominantly right-hand to a symmetrical distribution of right-hand and left-hand events. It is of interest to pursue this transformation to still lower frequencies where Faraday rotation requires that measurements be made from the vicinity of the planet itself. As is true of all radio sources, the polarization phenomenon is an important clue to the details of the actual radiation mechanism.

6. Background of the Investigators

The University of Florida Radio Observatory was one of the first university groups in the nation to engage in radio observations of the planets. The Observatory was, in fact, founded in 1956 by Professors A. G. Smith and T. D. Carr for this specific purpose. Since 1956 the Observatory has carried on a continuous program of monitoring Jupiter over the entire decametric range permitted by atmospheric conditions. During this period the program has resulted in 92 publications in the scientific literature and a total of 31 graduate degrees (21 M. S. and 10 Ph. D.'s) awarded to students involved in the research. Drs. Smith and Carr are co-authors of the only monograph devoted to planetary radio astronomy.

In 1959 a well-equipped southern hemisphere observatory was established at Maipu, Chile; this facility also has been devoted almost exclusively to decametric observations of Jupiter. It is continuously manned by Chilean personnel and supervised through periodic visits by Florida scientists. The Maipu observatory is funded jointly by NSF and the University of Chile. In 1965 a smaller field station was set up in the Chilean Andes near Huanta. Funded by NASA, this highly isolated station was designed specifically to provide ground-based coverage of Jupiter at the lowest possible frequencies for back-up of space experiments. Observatory personnel have maintained an active interest in space radio astronomy as a logical -- indeed, almost a necessary -- extension of their long experience in ground-based observations of Jupiter. The group has completed a $60,000 NASA-sponsored study of the requirements for an earth-orbital radiometer for this purpose, and a prototype has been constructed by a subcontractor; the present proposal has of course benefitted significantly from these studies, which extended over a 3-year period.

During 1967 the Florida observatory was moved from the Gainesville campus to a 60-acre tract in a noise-free rural area 50 miles west of Gainesville. Establishment of this new facility was made possible by an NSF Science Development Grant. University of Florida data on Jupiter now extend continuously over 13 years. All of the observational material has been reduced to punch-card form and is available, together with relevent solar and geophysical parameters, for any type of machine analysis.

The Observatory operates field stations for long-baseline interferometry at St. Petersburg, Florida (in cooperation with Florida Presbyterian College) and at Bowling Green, Kentucky (in cooperation with Western Kentucky University).

A bibliography of Observatory publications is attached. Complete details on the facilities and personnel are given in Section III and in Sections I and II of the Management document.

7. Interplanetary, Asteroid and Jovian Ionospheric Electron Density Measurements.

The primary need for the impedance measurements is to enable the radiometer measurements to be correctly related to antenna and source temperatures[1]. By analogy with similar experiments we have conducted from space vehicles in the Earth's ionosphere[2] it is evident that the corrections for impedance changes will be particularly important as the spacecraft enters the Jovian ionosphere; the impedance variations as a function of position along the spacecraft trajectory will be very marked.

The reactance part of the impedance can reverse sign completely, and its magnitude and that of the radiation resistance may both change by orders of magnitude. Extensive measurements of antenna impedance in the ionosphere have also been made by Miller and Schulte[3]. The reactance change from the free space value due to electron density changes are shown in the following table for operating frequencies of 26, 104, and 416 KHz. X_{A_o} is free space antenna reactance, X_A is the reactance in a cold plasma with negligible magnetic field index n. Then the ratio of reactance in this plasma to the reactance in free space is

$$\frac{X_A}{X_{A_o}} = n^{-2} = \left[1 + (f_p/f)^2 \right]^{-1},$$

where the plasma frequency $f_p = 9000\ N_e^{1/2}$ Hz, and N_e is the electron density per cm^3.

Table of Antenna Reactance Ratios for Various Values of Ambient Electron Density

X_A/X_{A_o}	$(f_p/f)^2$	Electron Density N_e (cm^{-3})		
		26 KHz	104 KHz	416 KHz
1.14	0.125	1	16	256
2.0	0.50	4	64	1024
∞	1.00	8	128	2048
-4.0	1.25	10	160	2560
-0.25	5.00	40	640	10240
-0.11	10.00	80	1280	20480

The above table displays values of N_e for the three operating frequencies which produce the five tabulated ratios of free-space antenna reactance to the reactance in a cold plasma with negligible magnetic field. Thus the experiment can detect electron density values from 1 to 20,480 cm^{-3}. The Michigan OGO-IV antenna impedance device can measure reactance ratios having these tabulated values.

REFERENCES:

1. Antenna Impedance in a Plasma: Problems Relevant to Radio Astronomy Measurements from Space Vehicles. by D. Walsh and F. T. Haddock. Extrait des Annales d'Astrophysique V28, N3 pp 605-613 1965.

2. Cosmic Radio Intensities at 1.225 and 2.0 MHz Measured up to an Altitude of 1700 KM. by D. Walsh, F. T. Haddock and H. F. Schulte Preceedings of the Fourth International Space Science Symposium, Warsaw, June 3 - 12, 1963.

3. Antenna Admittance in an Ionospheric-Type Plasma. E. K. Miller and H. F. Schulte, Jr., 1968. Presented at the NATO Advanced Study Institute on Plasma Waves in Space and the Laboratory, Roros, Norway.

IV. APPROACH

1. THEORETICAL MODELS DESCRIBING S BURST SOURCES

Flagg and Carr of the University of Florida have shown that the millisecond bursts are partially composed of trains of micropulses having widths of 20 μsec or less. It is not unusual for isolated micropulses to occur, producing events where total duration is measured in tens of microseconds.

The mechanism that is responsible for these millisecond bursts and micropulses is as yet quite unclear. Various models which have been proposed are

(1) a small, intensely active region which is activated by Io[1, 2]

(2) many small active regions which emit randomly[3]

(3) a large active region which radiates into very narrow beams, the bursts arising from the spatial sweeping of the beams over the antenna[4]

(4) a large active region which radiates narrow-band radiation, the bursts arising from the sweeping of this band across the spectrum[5].

The first model has the most support from ground-based experiments. If the microsecond pulses are to be explained as a result of the spectral sweeping described in model "4" sweep rates up to 5000 MHz/sec are required. While Warwick has detected sweep rates as high as 25 MHz/sec[5], none as high as 5000 MHz/sec have been detected. Measurements by Flagg and Carr (private communication) show that on this fast time scale, the existence of a micropulse at a given frequency by no means implies that one exists at a neighboring frequency as little as 200 KHz away; thus the mechanism for micropulses evidently is not that of a swept generator. Model "3" suggests that if a beam sweeps over the earth due to Jupiter's rotation, its angular width must be only 2×10^{-7} radian (0.04" of arc) if it is to sweep past the antenna in 20 μsec. It is

---

[1] Ellis, G. R. A. Radio Science, 69D, 1513, 1965

[2] Flagg, R. S. and T. D. Carr. Astrophysical Letters, 1, 47, 1967.

[3] Warwick, J. W. Private communication to F. Haddock.

[4] Warwick, J. W. Space Science Reviews, 6, 841, 1967.

[5] Warwick, J. W., and M. A. Gordon. Radio Science, 69D, 1537, 1965a.

possible to imagine that a beam might sweep faster in the north-south direction due to the acceleration of charged particles along Jupiter's magnetic field lines. Data from the University of Florida's long baseline interferometer predict that if the beam does sweep from north to south, its angular velocity must be over twenty times greater than that of Jupiter's rotation, since no systematic time delay greater than the timing uncertainty (0.2 msec) has been observed. Furthermore, to emit into such a narrow beam the source must be 75,000 km in diameter and must radiate coherently. Long baseline experiments conducted by Dulk[6] and Block[7] show that the source subtends less than 1" of arc at the earth or less than 0.03 Jupiter radius.

While there is no proof that model "2" is incorrect, it has never been formally proposed. It seems unlikely that when Io moves into a particular position, small, intense radio sources materialize over a volume of space comparable in size to Jupiter itself.

2. SOURCE LOCATION PROCEDURE

(1). Io-Related Emission -- Pulse Ranging Experiment

An experiment conducted at the University of Florida by R. S. Flagg and T. D. Carr showed that the millisecond (S) bursts and the microsecond (P) pulses which occur in Jupiter's decametric radio emission have rise times as short as 10 μsec or less. Since the occurrence of the S bursts and the pulses can be predicted from the position of Jupiter's innermost Galilean satellite, Io, they provide a highly precise time reference which can be used to determine the position of the radio source in a manner analogous to radar. The 20.75 MHz Jupiter emission will be monitored both at the spacecraft and at two of the University of Florida's three ground stations, which are located in Dixie County, Florida, Maipu, Chile, and Huanta, Chile. The primary Florida observatory will be backed up by the Huanta observatory, which is located in a interference-free Andean valley in northern Chile. The Huanta site, which is located at 30° south latitude, will be particularly favorable during 1972-1973, since Jupiter's declination will be between

---

[6] Dulk, G., B. Rayher, and R. Lawrence. Ap. J. Letters, 150, L117, 1967.

[7] Block, W. F., et al., SE Sec, APS, Athens, Ga., Oct. 9-11, 1968.

15° and 23° south. If a third field station were located near the NASA tracking facility in Carnarvon, Australia, the ground observing time could be doubled, giving essentially full earth-based coverage of Jupiter.

A 20.75 MHz frequency was chosen for the primary source location experiment, since Jupiter radiates intensely at that frequency while terrestrial interference is minimized. Two 20.75 MHz receivers have already been constructed for the ground-based part of the experiment. However, since the satellite back-up receivers are useful over a wide range of frequencies, the source ranging experiment can be repeated at several frequencies above the ionospheric cut-off as a means of determining whether the position is a function of frequency. Figure IV-12 shows the predicted flight.

During a ranging experiment, the precise time of arrival of each burst at the ground (T_2) and at the spacecraft (T_1) will be recorded. These two sequences of time will be cross-correlated to determine the difference in time of arrival of the bursts at the spacecraft and at the earth. Determination of this difference in time of arrival ($T_2 - T_1$) will allow one to place the source somewhere in space on a hyperboloid of revolution, as shown in Figure IV-1. (Note that the origin for this coordinate system lies midway between the spacecraft and the earth.) Subsequent measurements will yield different values for ($T_2 - T_1$), due to the relative motion of the spacecraft, Jupiter and the earth. The intersections of these hyperboloids will locate the source uniquely with respect to Jupiter.

(2). Emission Characteristics

Jovian decametric radiation is commonly classified as either L or S burst activity. L-burst activity, which predominates, is characterized by changes in signal amplitude which occur on a time scale of 0.1 to 10 sec. S-burst activity is characterized by short energy bursts, each burst generally having a duration of several milliseconds. The burst repetition rate is highly variable, lying between extremes of approximately 5 and 50 bursts per second.

Figure IV-2 shows typical examples of both L and S burst activity. The subclassifications of S-burst activity (S_1 and S_2) are arbitrary and may be thought of as representative of the mean and extreme burst

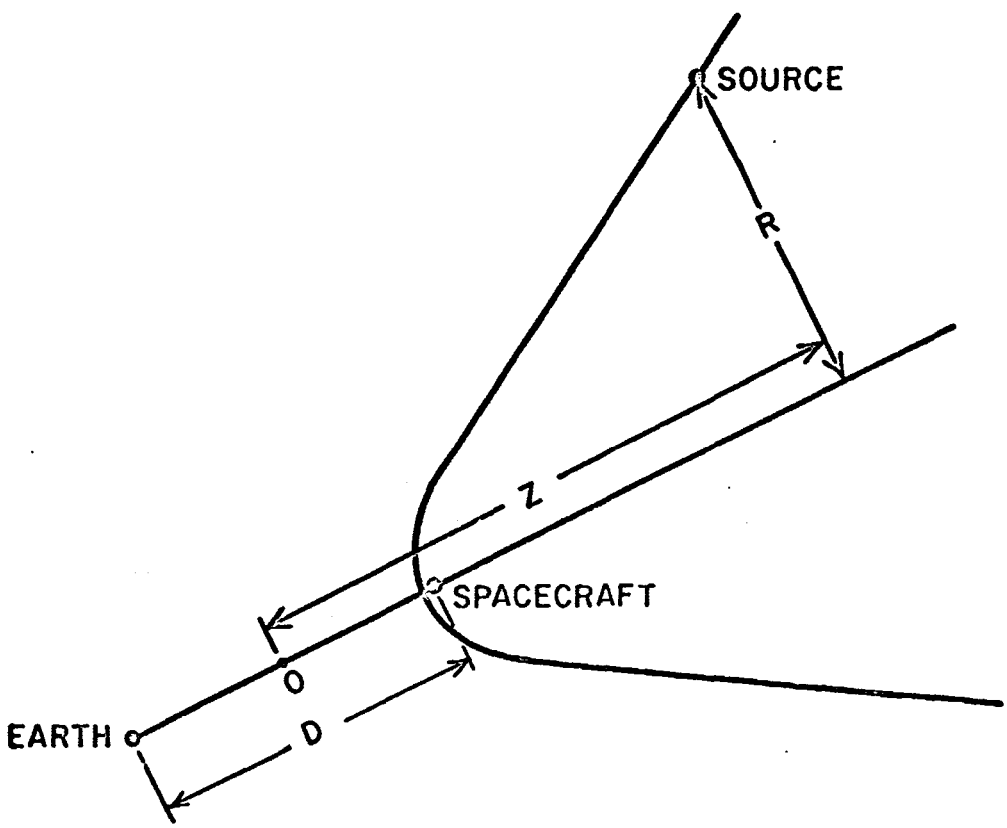

$$\frac{Z^2}{\left[\frac{V}{2}(T_2-T_1)\right]^2} - \frac{R^2}{\left(\frac{D}{2}\right)^2-\left[\frac{V}{2}(T_2-T_1)\right]^2} = 1$$

Figure IV-1. The earth-source-spacecraft configuration showing the locus of points (hyperboloid) on which the source must be for a given $(T_2 - T_1)$.

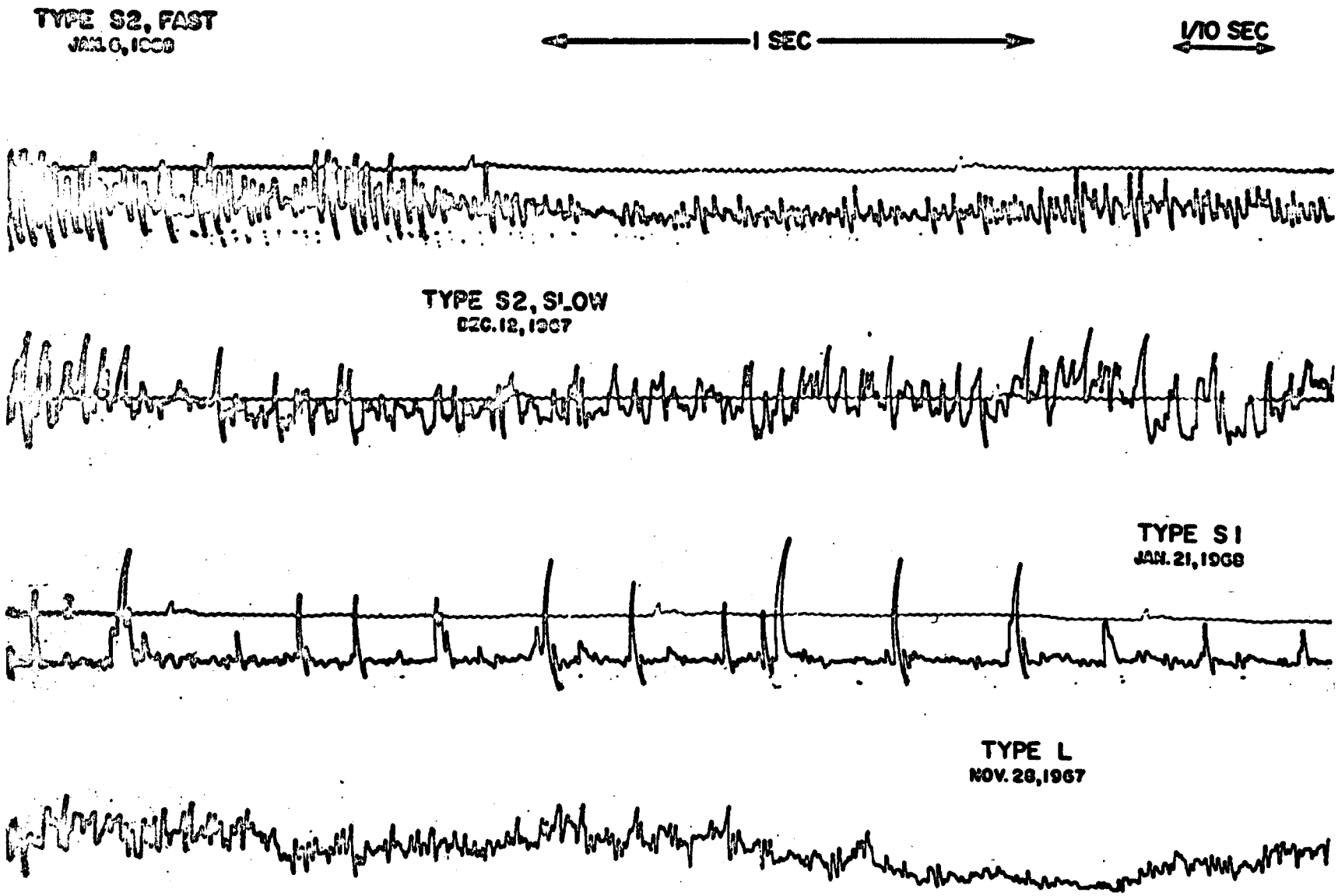

Figure IV-2. Typical examples of Jovian L- and S-burst activity.

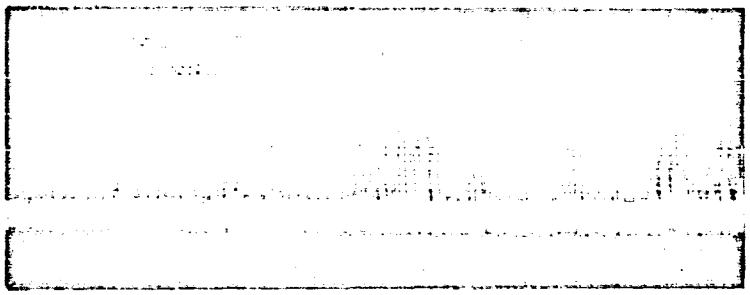

A. 5 mm/sec

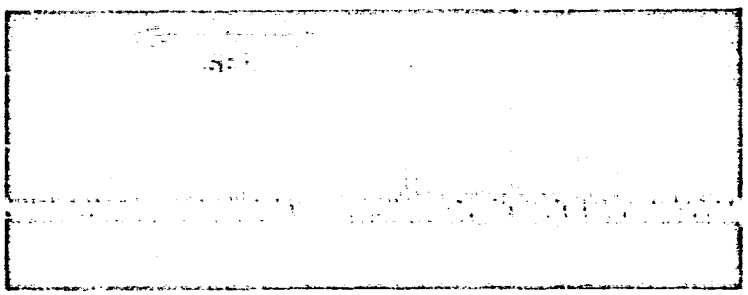

B. 25 mm/sec

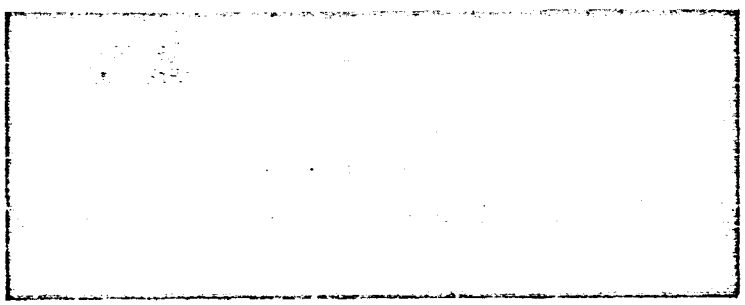

C. 125 mm/sec

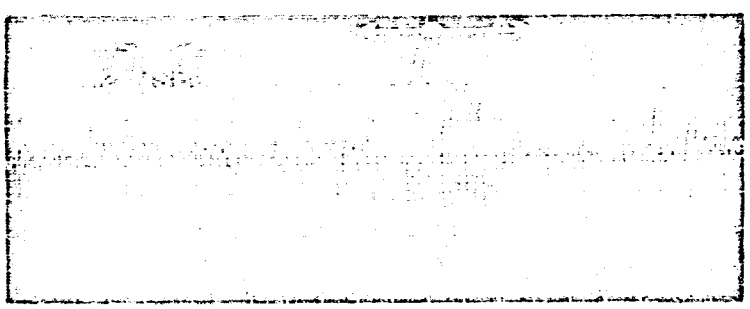

D. Slowed down 100:1
Recorded at 25 mm/sec

Figure IV-3. Typical S-burst activity recorded with increasing time resolution. The dot marks the same burst on each record.

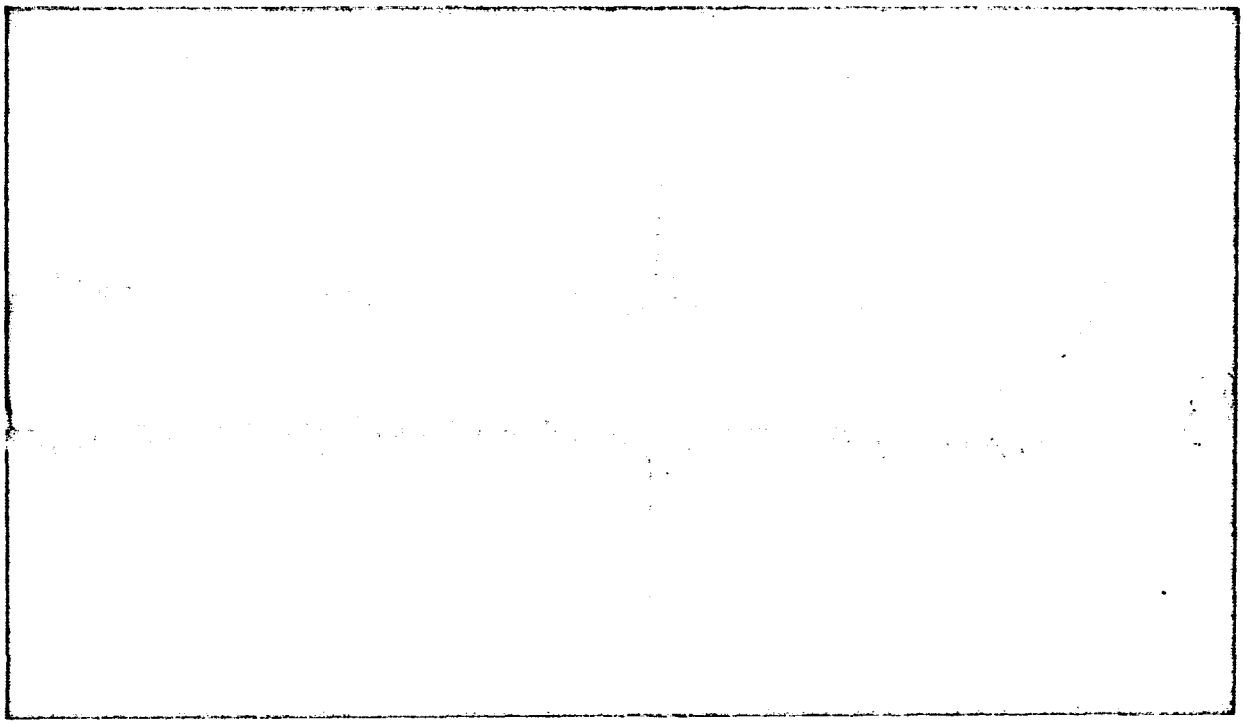

Figure IV-4. Isolated 30-microsecond pulse on 2000 μsec sweep.

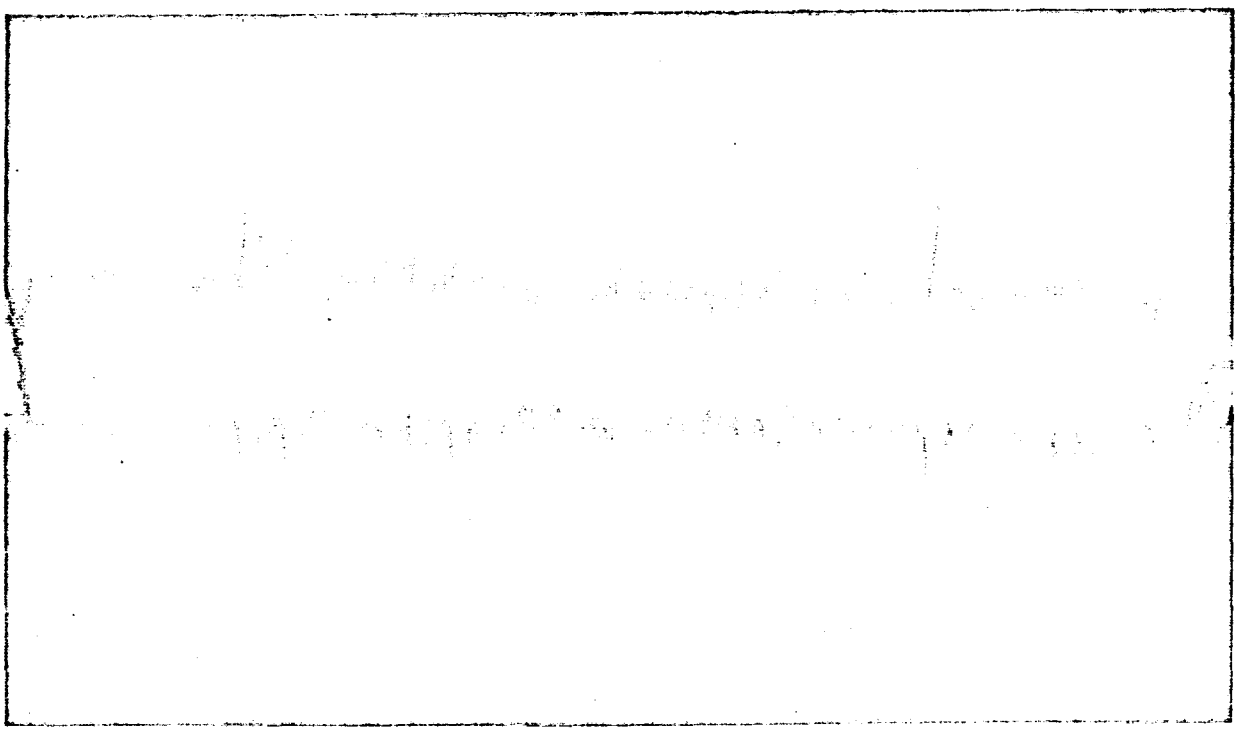

Figure IV-5. Two isolated 30-microsecond pulses with 2000 μsec sweep.

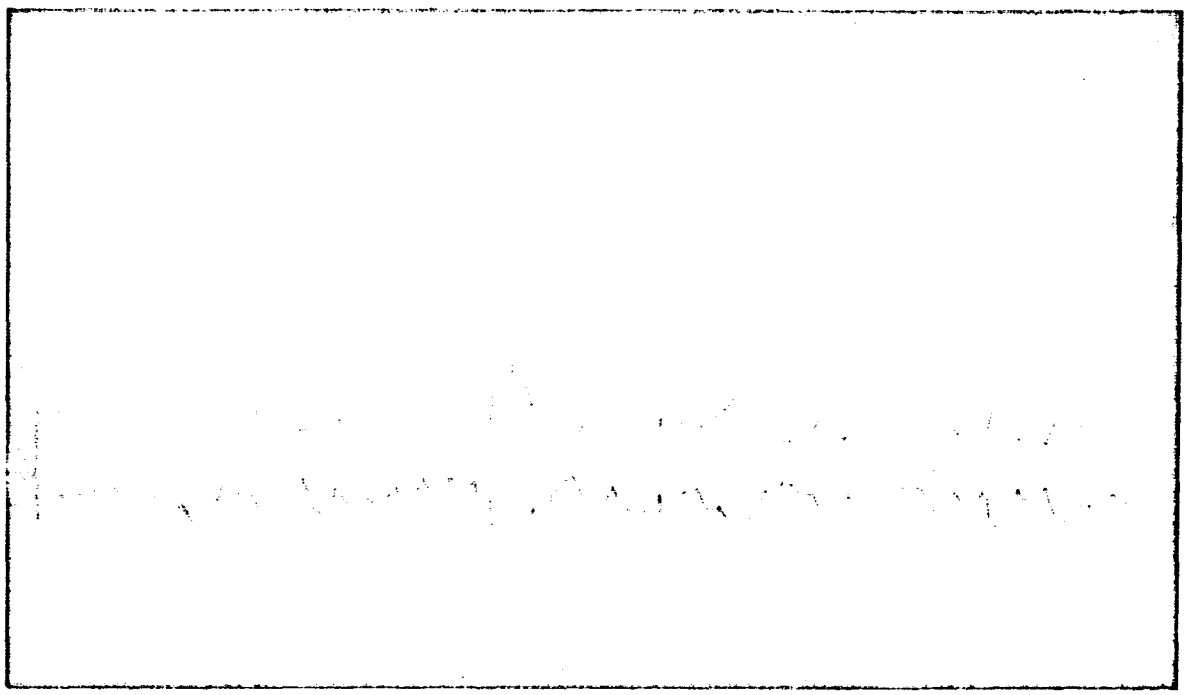

Figure IV-6. Isolated 30-microsecond pulse with 500 μsec sweep.

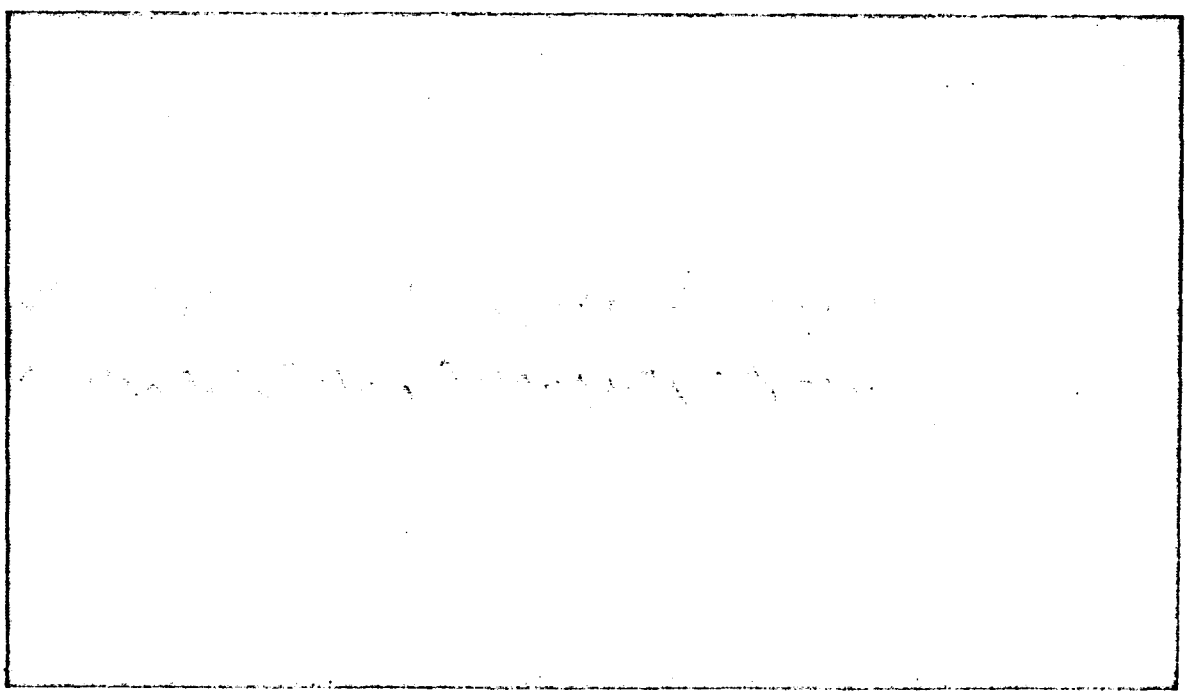

Figure IV-7. Isolated 30-microsecond pulse group on 500 μsec sweep.

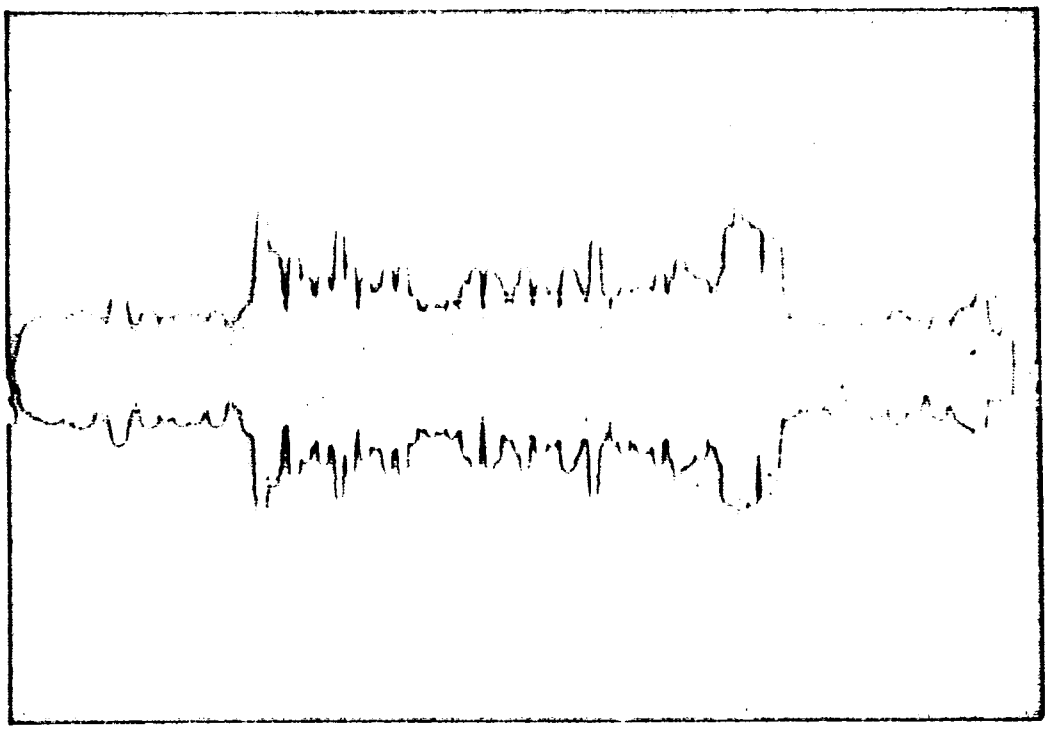

Figure IV-8. S-burst with 2000 μsec sweep.

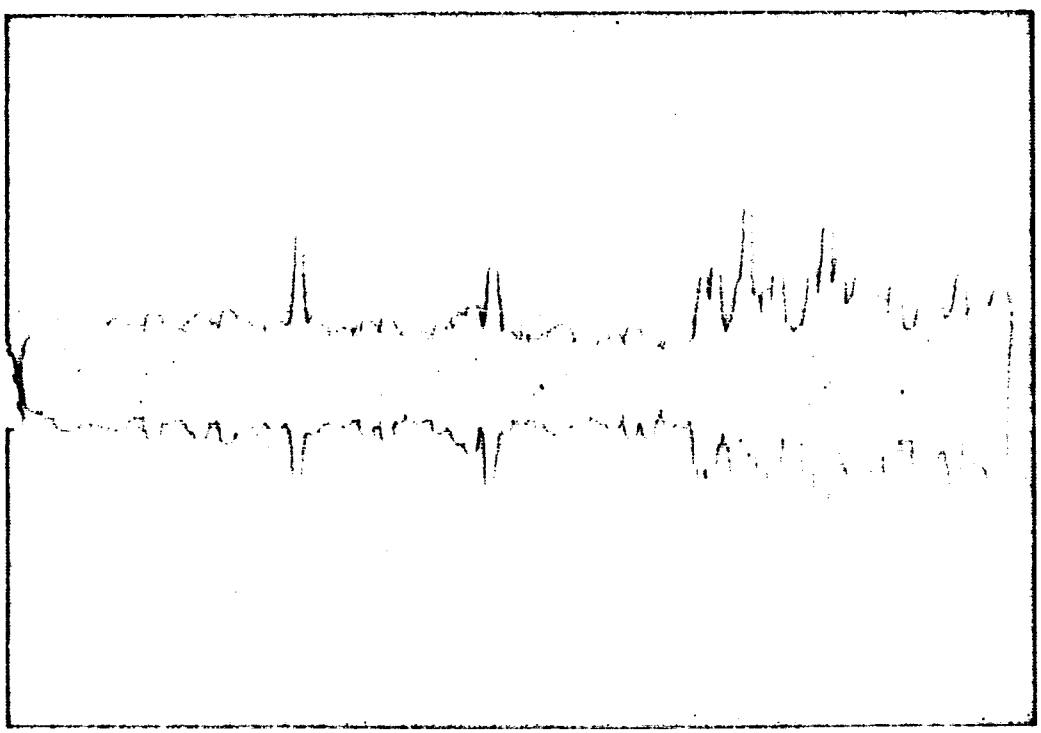

Figure IV-9. Isolated 30-microsecond pulses and beginning of S-burst on 2000 μsec sweep.

rates. In Type S_1 emission, (low burst repetition rates) the bursts sometimes appear to be periodic over intervals of 4 or 5 bursts, while the characteristically fast S_2 bursts seem to be randomly spaced. At times S-burst and L-burst activity occur simultaneously, producing slow amplitude modulation on the millisecond bursts.

Figure IV-3 shows several records of a typical period of Type S_1 activity. The A, B, and C portions were produced by playing the tape-recorded audio output of the receiver into a strip chart recorder at chart speeds of 5, 25, and 125 mm/sec, respectively. These data are bandlimited by the strip chart recorder, which has a frequency response from dc to 100 cps.

The D portion was produced by slowing down the tape data by a factor of 100, and then playing it into the strip chart recorder running at a speed of 25 mm/sec. These data are bandlimited by the 2.5 KHz receiver bandwidth; hence, the time resolution of the data in D is 0.4 milliseconds. The burst shown in D has a duration of 10 msec. The predominant frequency component within the envelope is 1.25 KHz, the center of frequency of the product-detected receiver output.

Figure IV-8 shows a single Jovian S burst recorded by photographing a cathode-ray tube on which was displayed the undetected IF output of a 22.2 MHz receiver having a 3^{db} bandwidth of 100 KHz. The burst duration is 1.07 msec. and the leading and trailing edges appear to be bandlimited to a time resolution of 10 microseconds.

Figure IV-9 is another example of Jovian S burst activity recorded with the 100 KHz bandwidth system. The beginning of a burst, as well as two isolated pulses, are seen. Isolated pulses, which have durations on the order of 30 μsec., occur frequently during periods of Jovian S-burst activity. The statistics pertinent to the S bursts and pulses are discussed in the following section.

The bursts themselves appear to be composed of both bandlimited Gaussian noise and the 20-40 microsecond pulses. Figures IV-4, IV-5 IV-6, and IV-7 show further examples of these pulses. These pulses and/or the S bursts will provide the accurate time reference needed to perform the pulse ranging experiment. The average pulse character will be monitored using the burst characteristics experiment discussed in Section IV-6.

(3). Emission Statistics

A brief analysis of Jovian bursts from a typical sample of data obtained during the 1966-1967 apparition is shown graphically in Figures IV-10 and IV-11. Thirty-eight S_1 bursts having durations greater than 1 msec are shown in the plots. In addition to these bursts, an additional 53 bursts with durations less than 1 msec were recorded over the same 3-second sampling interval. The average burst rate over the entire interval is 30 bursts/sec. The a and b portions of the figures were derived from those bursts which exceeded the 3 RMS and 6 RMS galactic noise levels respectively. The results show that the burst durations for the 38 bursts studied in detail range from 1 to 70 msec. For those bursts exceeding the 3 RMS level the average duration is 14.7 msec with a standard deviation of 16.8 msec. The durations of those bursts exceeding 6 RMS level range from 1.0 to 46 msec with an average of 13.2 msec and a standard deviation of 12.5 msec. The distribution of rise times for these bursts is shown in Figure IV-11. For bursts exceeding the 3 RMS and 6 RMS levels the average rise times are 1.5 msec (standard deviation 2.1 msec) and 7.0 msec (standard deviation 7.9 msec), respectively.

Finally, an additional analysis was made to determine the isolated Jovian pulse rate. The data were obtained using a 100 KHz bandwidth receiver. A total of 409 pulses was received during a 4.159 sec. sampling interval, yielding an average pulse rate of 98 pulses/sec. Pulse rates during the sampling interval ranged from 50 to 150 pulses/sec.

(4). Fundamental Limitations

If precise position measurements are to be made, the following parameters must be known or measured accurately: 1. The time of pulse arrival at the earth (T_2) and at the spacecraft (T_1); 2. The velocity of light en vacuo (C); 3. The velocity of 20.75 MHz electromagnetic waves in interplanetary space (v); and 4. The position of the spacecraft (D). Uncertainties in these parameters lead to errors in the source position measurement. However, the error in the position also depends on the geometrical relationship between the earth, the spacecraft, and Jupiter. For this reason a simple 637-day transfer orbit was calculated using a launch date of March 4, 1972. The pertinent orbital parameters are listed below:

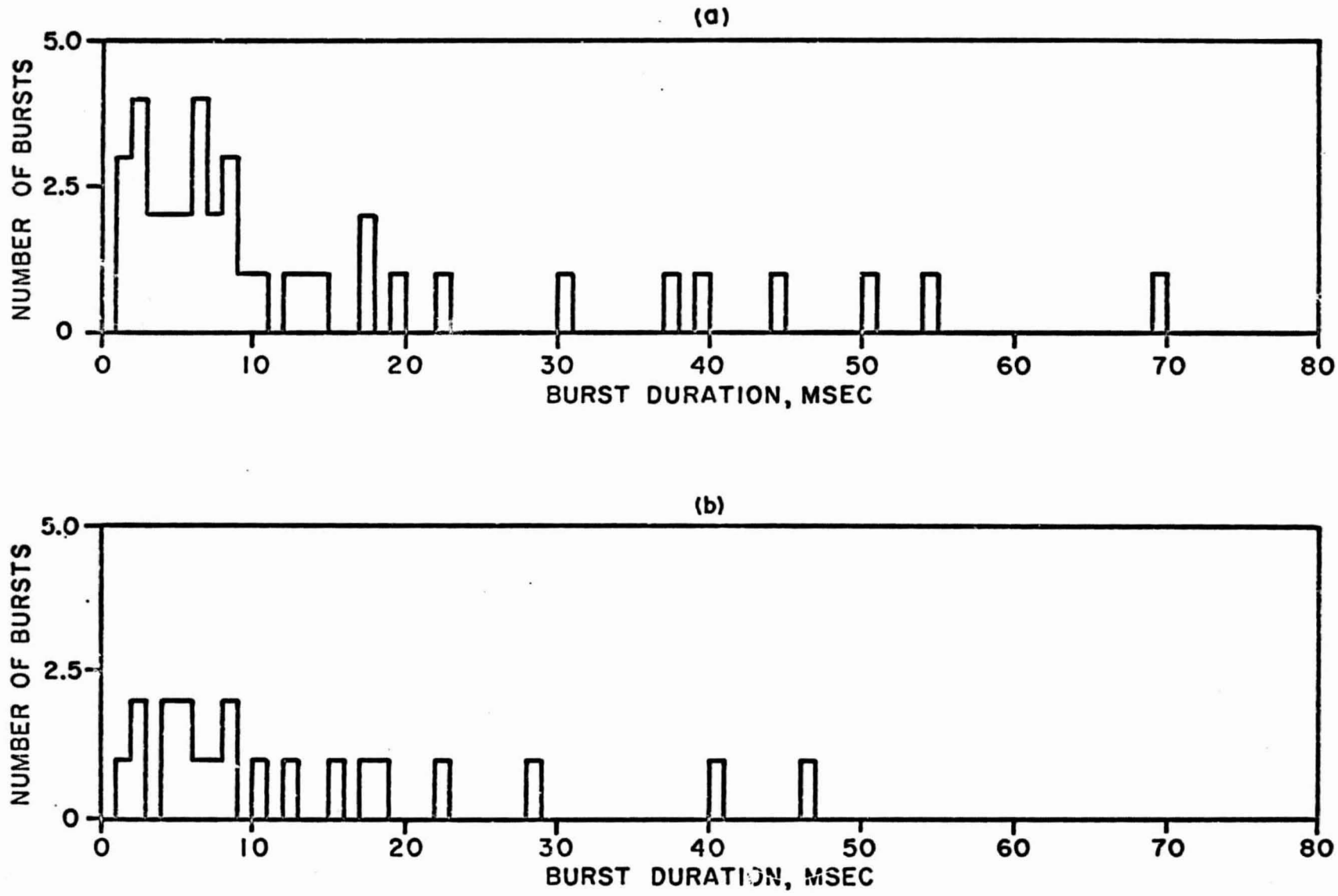

Figure IV-10. (a) Burst duration above a 3 RMS background. (b) Burst duration above a 6 RMS background.

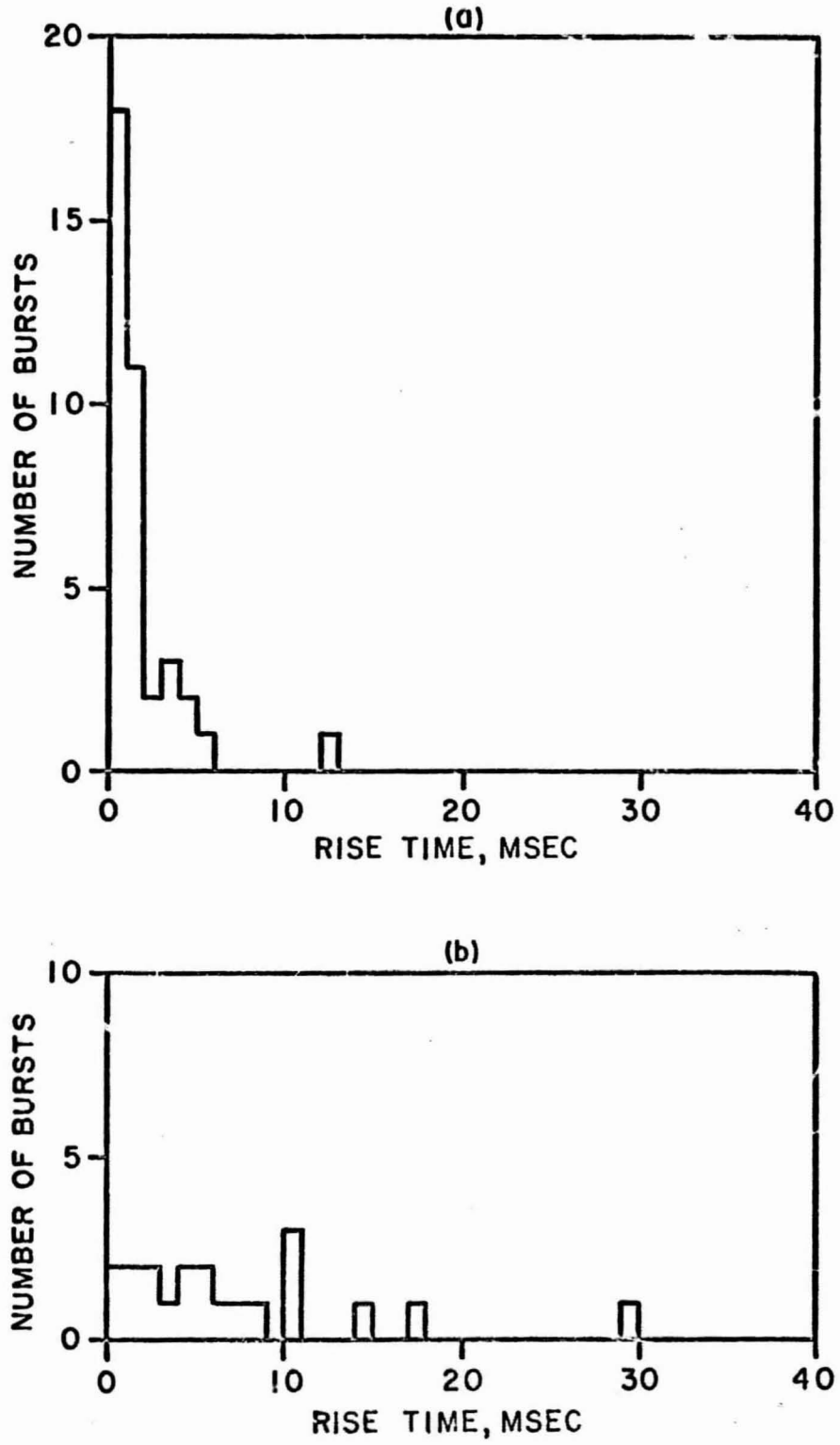

Figure IV-11. (a) Rise time to a 3 RMS background level.
(b) Rise time to a 6 RMS background level.

	Earth	Jupiter	Spacecraft
eccentricity	0.01673	0.04816	0.71356
time of perihelion	1972.008	1963.74	1972.1644
semi-major axis (A.U.)	1.0000	5.203	3.4581
period (years)	1.0000	11.86	6.4307
ω (heliocentric longitude of perihelion)	103°0	13°84	159°85

Figure IV-12 shows these orbits as a function of time. Figures IV-13, IV-14, and IV-15 show the orbital configurations and the positions of the hyperboloid loci at launch plus 100, 160, and 460 days, respectively.

1. Timing

The accuracy with which the time of arrival of a pulse at the spacecraft (T_1) and at the earth (T_2) can be measured is limited by the pulse rise time and by timing errors. To maintain the spacecraft clock within an acceptable error of 10^{-4} sec of the same earth-time for two years, it must be referenced to a stable earth-based standard clock via telemetry. Relativistic effects alone would dilate the spacecraft time more than 40 msec during the 637 day transit period. Even the most stable ground-based clocks will drift about 50 μsec in 637 days.

If an accurate spacecraft clock is not available it would be possible to put timing on the data after they reach the ground station if one knows the spacecraft transmission delay increment. It would, however, be desirable to have accurate absolute timing available at the spacecraft. The variations of Z(ΔZ) and R(ΔR) with time from launch are shown in Figure IV-16 (see curves C and D), assuming a timing uncertainty (ΔT) of 10^{-4} sec.

2. Velocity of Propagation

The velocity of propagation of the 20.75 MHz emission depends on the interplanetary electron density (n). If n is assumed to be 6 electrons/cc at the earth's orbit and drops off as $1/r^2$, the propagation time of 20.75 MHz radio waves from Jupiter to the earth at the time of opposition differs from the free-space time by 0.2 msec. This leads to an uncertainty in the average velocity of propagation of 0.025 km/sec. The propagation time through the earth's night-time ionosphere adds another 0.2 msec to the propagation decrement. The net effect, then, of all the electrons

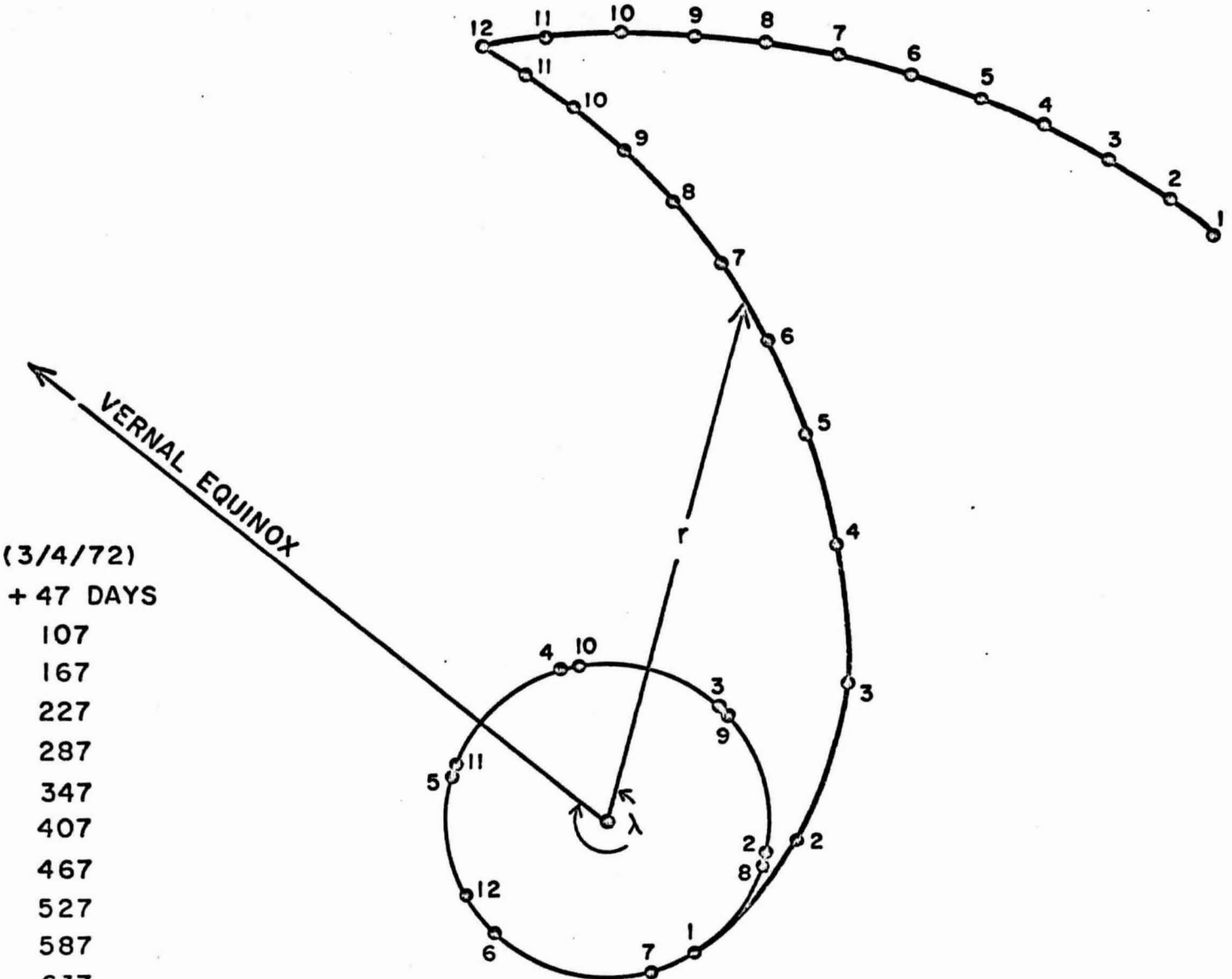

Figure IV-12. Orbits of the earth, Jupiter, and the satellite as a function of time.

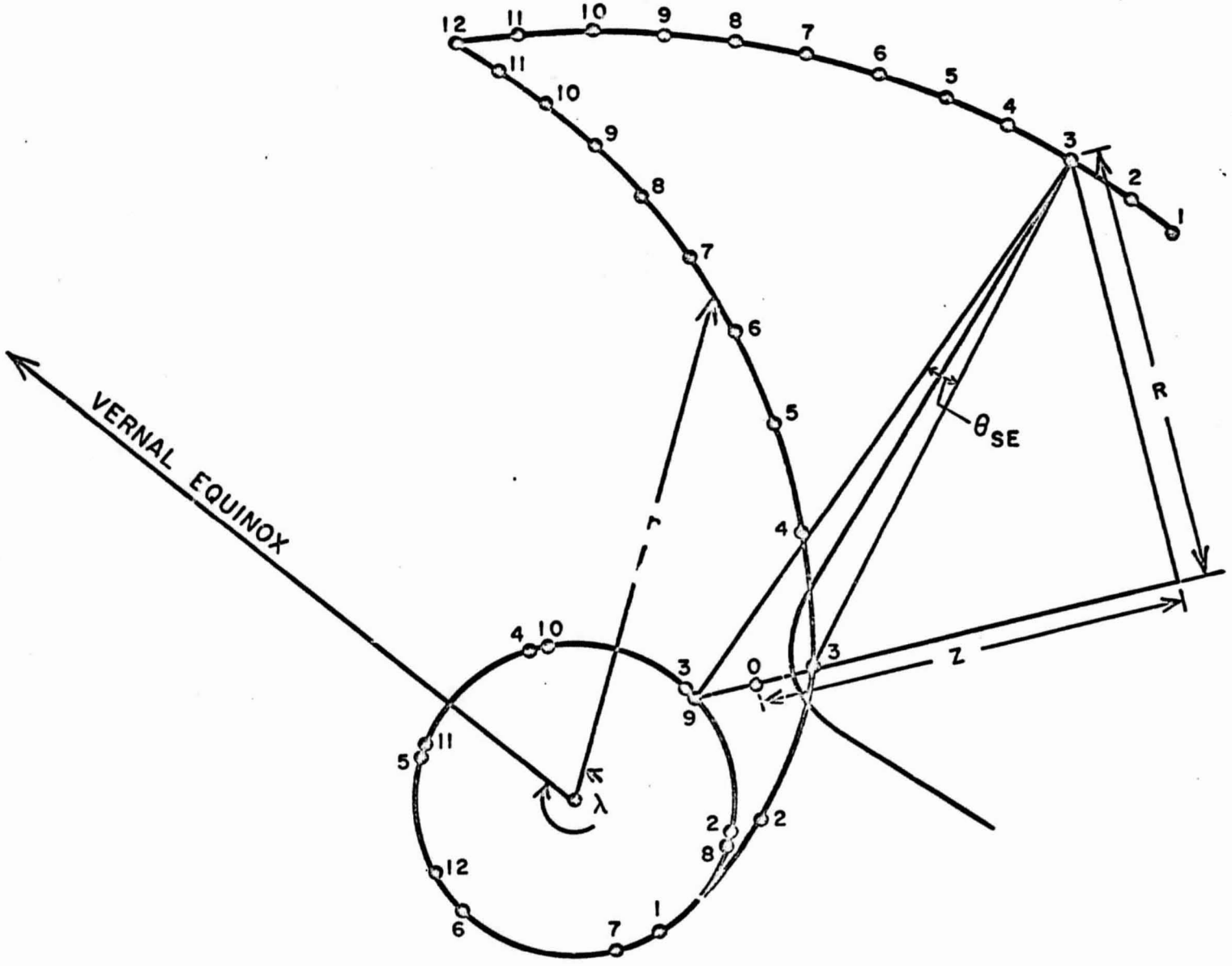

Figure IV-13. Orbital configuration and the position of the hyperboloid locus at launch plus 100 days.

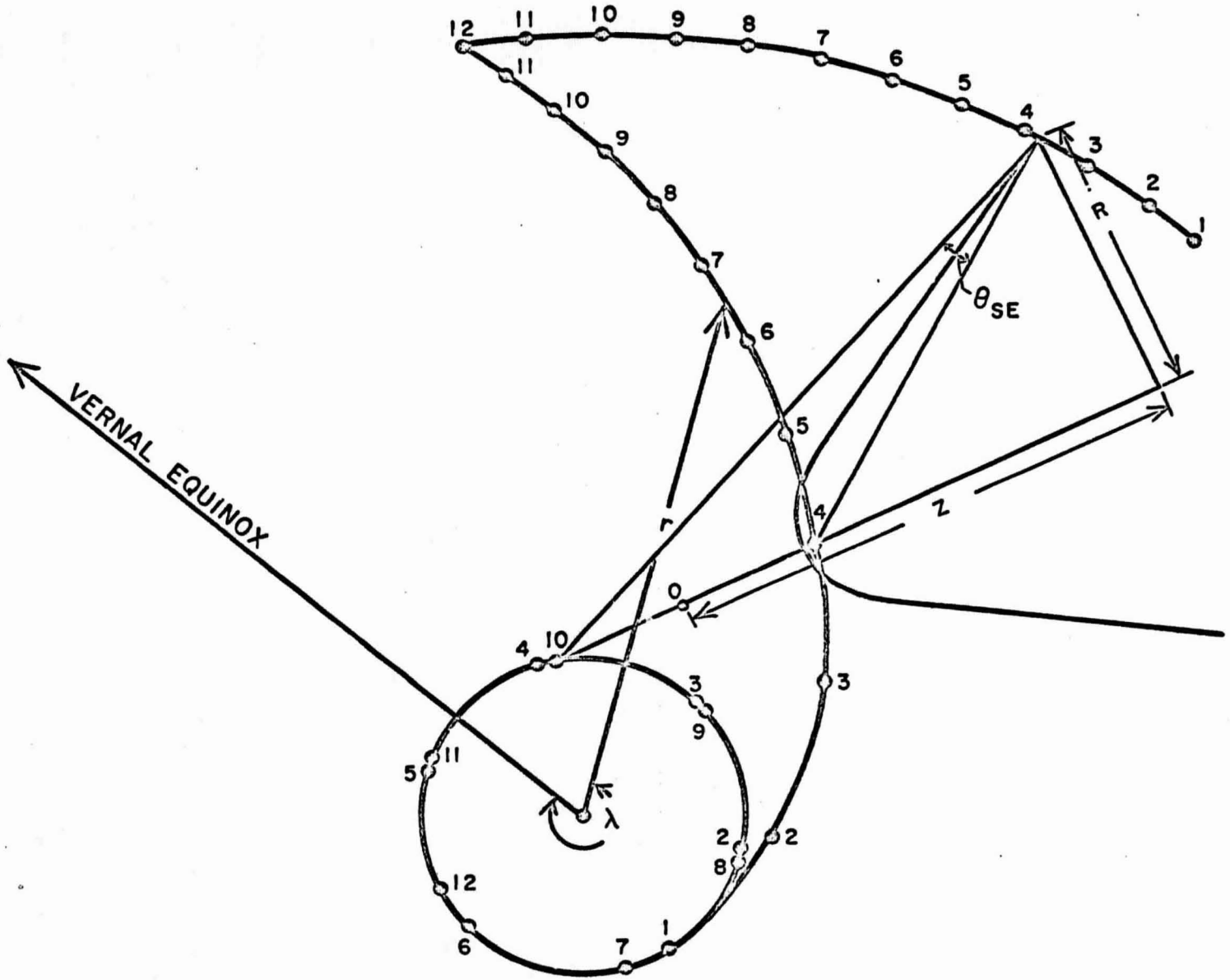

Figure IV-14. Orbital configuration and position of the hyperboloid locus at launch plus 160 days.

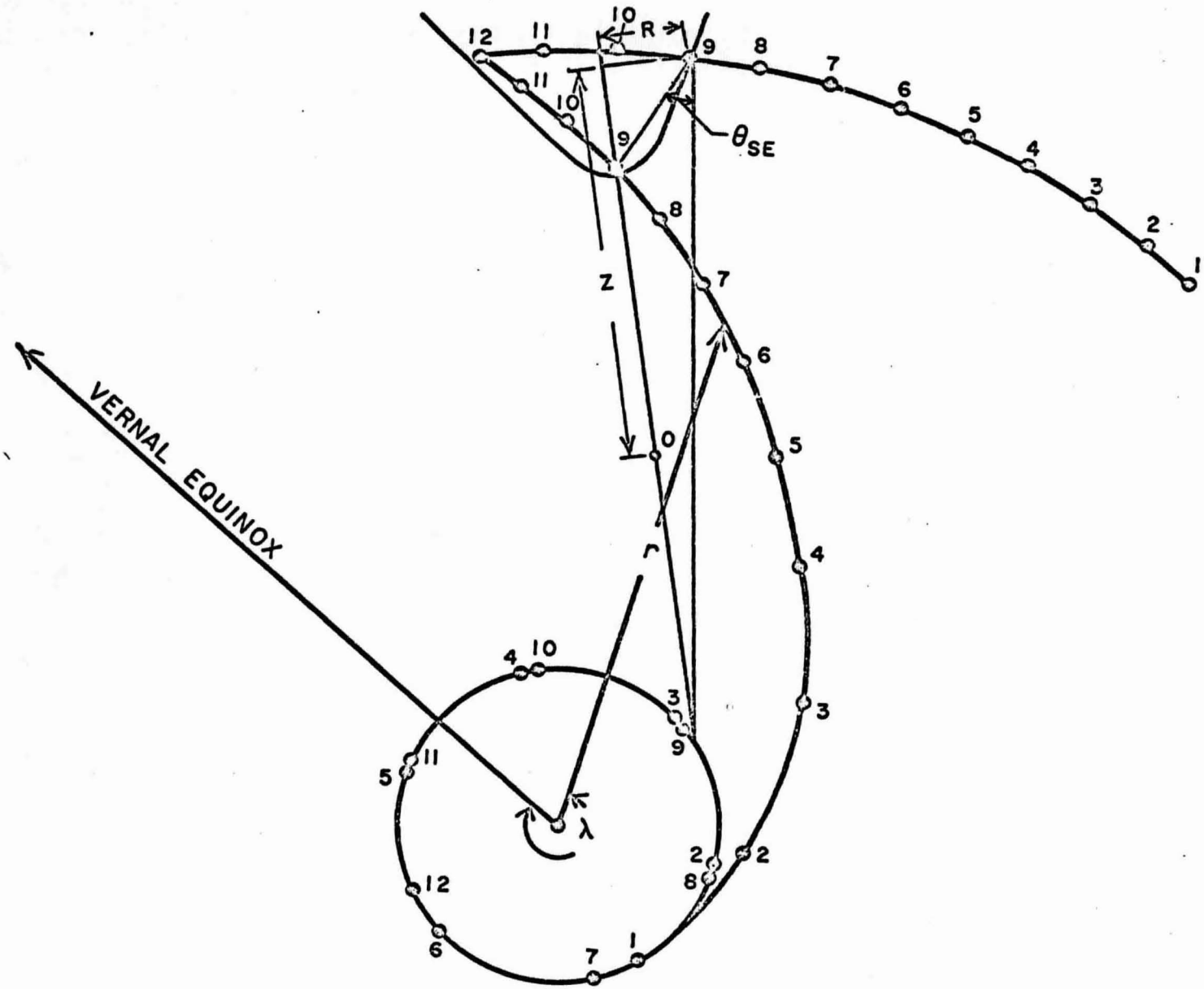

Figure IV-15. Orbital configuration and position of the hyperboloid locus at launch plus 460 days.

from Jupiter to the surface of the earth at the time of opposition is $\Delta v = c - v = 0.05$ km/sec. Curves A and B in Figure IV-16 show the respective uncertainties that arise in Z and R due to a propagation uncertainty Δv. Figure IV-17 is a comparison of the variations (ΔZ and ΔR) in the source location parameters (Z and R). Curves A and B show the effects of Δv on ΔZ and ΔR, respectively; and curves C and D show the variations in ΔZ and ΔR due to a timing uncertainty ΔT. A timing uncertainty $\Delta T = 10^{-4}$ sec and a propagation decrement $\Delta v = 0.03$ Km/sec yield the same value for ΔR. Since Δv is approximately 0.025 km/sec the timing errors and propagation errors are about equal if the timing uncertainty is 10^{-4} sec. However, with the help of a radio propagation experiment, Δv can be reduced considerably. Figure IV-16 shows that the source can be located to less than 1000 km, or less than 1% of the planet's diameter. Between 370 and 550 days past launch the position determination is accurate to less than 300 km. Note that the most precise source position measurements can be made when θ_{SE} (the earth-spacecraft angle as seen from Jupiter) is largest. Curve E in Figure IV-16 shows θ_{SE} as a function of time.

Figure IV-16 also shows that at about 278 days from launch the satellite will pass between the earth and Jupiter, making θ_{SE} zero. At this time ranging experiments will be of little value, since ΔR and ΔZ are very large. However, the difference in time of arrival of the pulses at the spacecraft and at the ground will yield a direct measurement of the total electron content in the earth-spacecraft line, a result that can be compared with the value found from a radio propagation experiment. Figure IV-16 shows that at 278 days past launch the earth-spacecraft line passes within about 0.4 A. U. of the sun, making possible an independent measurement of coronal electron density.

Figure IV-16 shows that two periods during the flight will be especially favorable for the pulse-ranging experiment; one is early in the flight (70-200 days), the other late in the flight (400-500 days). Both periods fall around opposition, when ground-based observations can best be made. The first period is preferred for three reasons: one, the spacecraft is close to the earth so that high telemetry bit rates are possible; two, significant experimental results relating to Jupiter will be obtained early in the flight; and three, the beaming angles will be small at this time. It is highly desirable that some

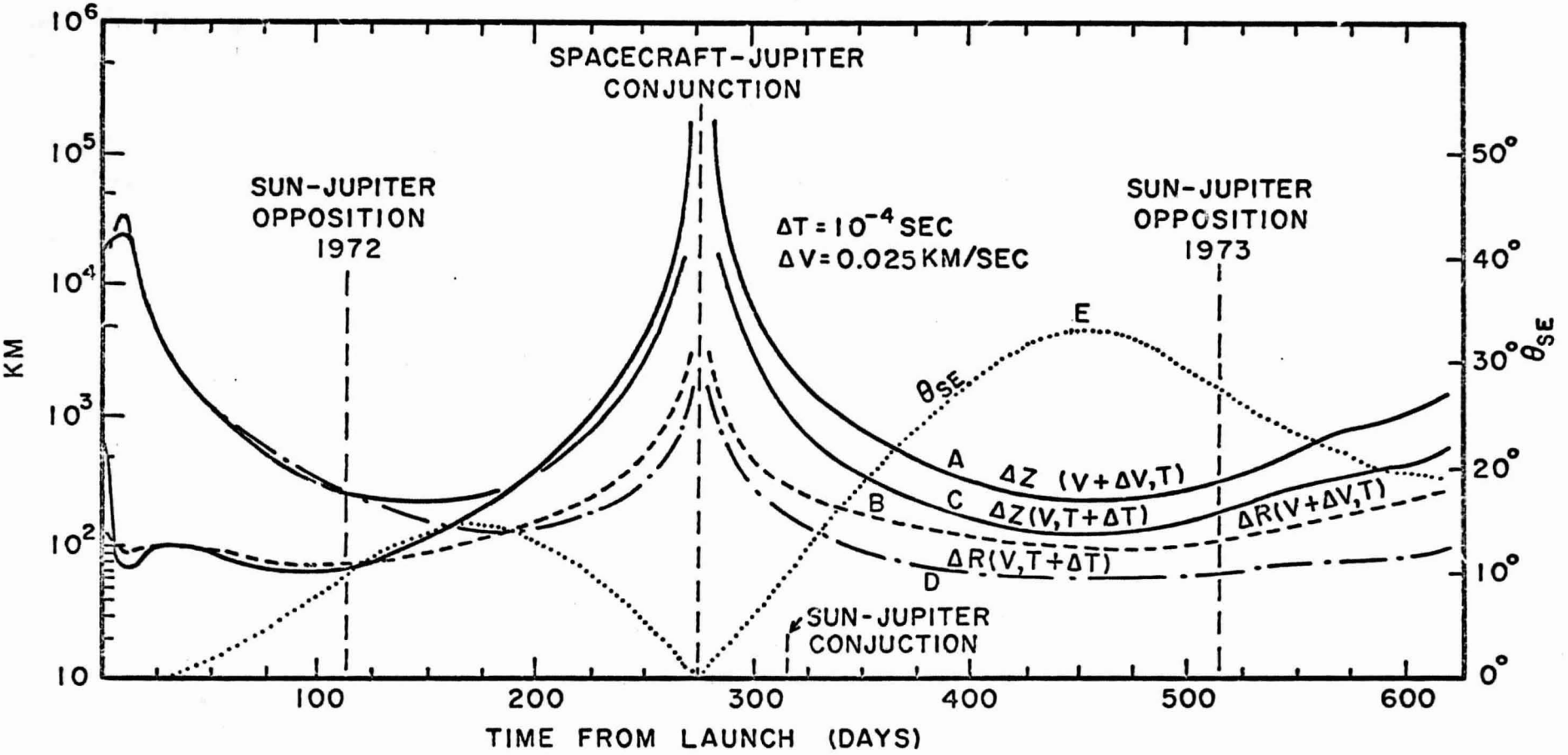

Figure IV-16. ΔR and ΔZ as a function of time from launch for Δv = 0.025 km/sec (curves A and B) and for $\Delta T = 10^{-4}$ sec (curves C and D). Curve E shows θ_{SE} as a function of time.

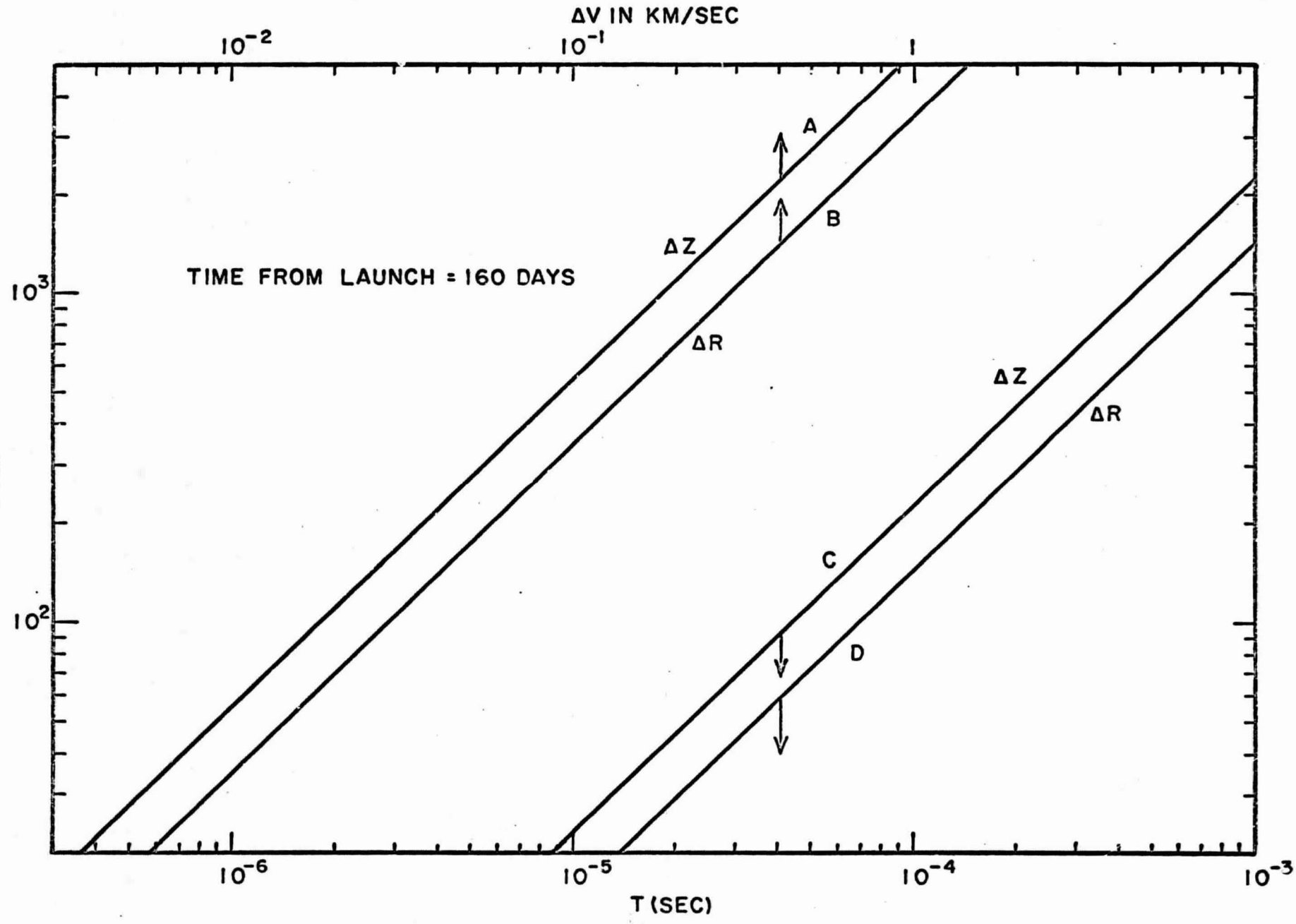

Figure IV-17. Comparison of the variations (ΔZ and ΔR) in the source location parameters (Z and R).

of the Jupiter-related experiment goals be realized even if the actual encounter should prove unsuccessful. However, the signal-to-noise ratio of the Jupiter signals at the spacecraft will be greater and ranging will be more precise in the 400-500 day period. Io-related events observable from the Florida or Chilean observatory during each of these periods can be read from the predictions in Table IV-1.

3. Spacecraft position

The equation in Figure IV-1 shows that the earth-spacecraft distance affects the definition of the hyperboloid. Therefore, it is urged that the spacecraft position be specified as accurately as possible.

4. Geometrical Dilution of Precision

Discussion earlier in this section indicates that the source will lie at the intersection of two hyperboloids defined by different earth-source-spacecraft geometries. However, if the assymptotes are nearly parallel the precision of the parameter Z is reduced. The hyperbolas in Figures IV-14 and IV-15 intersect at an angle of 20°. Figure IV-16 shows that $\Delta Z \simeq \Delta R \simeq 300$ km at launch plus 100 days, making the maximum error in Z approximately $10^3/\sin 20° \simeq 1000$ km and the error in R approximately $10^3/\cos 20° \simeq 330$ km. However, if Jupiter's radiation beam were very narrow, hyperbolas would be defined only when the spacecraft and Jupiter are near conjunction. To consider an unrealistically unfavorable case, if the beam were only 1° wide the largest angle of intersection of any two measurable hyperbolas would be 2°, yielding an uncertainty in Z of $10^3/\sin 2° \simeq 3 \times 10^4$ km, which is still less than one Jupiter radius. There is, however, no reason to expect such an unfavorable geometry.

5. Correlation Time

Determination of the difference-in-time-of-arrival parameter $(T_2 - T_1)$ requires that one correlate the sequence of pulse times (T_{2_i}) measured at the earth with that from the spacecraft (T_{1_i}). However, the correlation coefficient will be diluted if the source moves 10^3 km or more during the time the sequence is being monitored. In the following section methods of optimizing the sampling technique are discussed. If the telemetry rate is 512 BPS, and if no spurious pulses are present, enough pulses will be collected in 5 seconds to calculate a reliable cross-correlation function. However, since the required correlation

TABLE IV-1. PREDICTED TIMES OF IO-RELATED EMISSION DURING THE PERIOD 4 MARCH, 1972 TO 1 DECEMBER, 1973.*

Date	Time, U.T.	Io Related Source
03-16-72	0430	A
03-23-72	0500	A
03-30-72	0600	A
03-30-72	0830	C
03-31-72	0900	B
04-06-72	0900	C
04-07-72	0930	B
04-13-72	1000	C
04-14-72	1030	B
04-17-72	0100	A
04-24-72	0130	A
04-29-72	1030	A
05-01-72	0000	C
05-02-72	0500	B
05-08-72	0530	C
05-09-72	0600	B
05-15-72	0600	C
05-31-72	0630	A
06-02-72	0100	C
06-03-72	0130	B
06-07-72	0730	A
06-09-72	0130	C
07-02-72	0300	A
07-09-72	0330	A
07-16-72	0630	C
07-17-72	0700	B
07-23-72	0730	C
08-10-72	0200	C
08-11-72	0230	B
08-15-72	0830	A
08-17-72	0300	C
08-18-72	0330	B
08-22-72	0930	A
08-24-72	0330	C
08-25-72	0400	B
09-09-72	0400	A
09-16-72	0500	A
09-23-72	0530	A
09-23-72	0800	C
09-24-72	0830	B
09-30-72	0900	C
10-01-72	0930	B
10-07-72	0930	C
10-08-72	1000	B
10-18-72	0100	A
10-23-72	1000	A
10-25-72	0200	A
10-25-72	0430	C
10-26-72	0500	B
11-01-72	0500	C
10-02-72	0530	B
11-08-72	0600	C
11-09-72	0630	B
11-24-72	0630	A
11-26-72	0100	C
11-27-72	0100	B
12-01-72	0700	A
12-03-72	0130	C
12-04-72	0200	B
12-08-72	0800	A
12-26-72	0230	A
01-02-73	0330	A
01-09-73	0630	C
01-10-73	0700	B
01-16-73	0730	C
01-17-73	0800	B
02-04-73	0230	B
02-08-73	0830	A
02-10-73	0230	C
02-11-73	0330	B
02-15-73	0930	A
02-17-73	0330	C
02-18-73	0400	B

* The events are those which will occur between 1800 and 0600 EST and will be suitable for observation from the Florida Observatory.

Date	Time, U.T.	Io Related Source
03-05-73	0400	A
03-12-73	0500	A
03-19-73	0530	A
03-20-73	0830	B
03-26-73	0830	C
03-27-73	0900	B
04-02-73	0930	C
04-03-73	1000	B
04-13-73	0100	A
04-20-73	0130	A
04-20-73	0400	C
04-21-73	0430	B
04-27-73	0500	C
04-28-73	0530	B
05-04-73	0530	C
05-20-73	0600	A
05-22-73	0100	C
05-23-73	0100	B
05-27-73	0700	A
05-29-73	0100	C
05-30-73	0130	B
06-03-73	0730	A
06-03-73	0900	C
06-05-73	0200	C
06-21-73	0230	A
06-28-73	0300	A
07-05-73	0400	A
07-05-73	0630	C
07-06-73	0700	B
07-12-73	0700	C
07-13-73	0730	B
07-19-73	0800	C
08-04-73	0830	A
08-06-73	0230	C
08-07-73	0300	B
08-11-73	0900	A
08-13-73	0330	C
08-14-73	0400	B
08-18-73	1000	A
09-05-73	0430	A
09-12-73	0530	A
09-19-73	0830	C
09-20-73	0900	B
09-26-73	0930	C
09-27-73	1000	B
10-07-73	0100	A
10-14-73	0130	A
10-14-73	0400	C
10-15-73	0430	B
10-21-73	0430	C
10-22-73	0530	B
10-28-73	0530	C
10-29-73	0600	B
11-13-73	0600	A
11-16-73	0100	B
11-20-73	0700	A
11-22-73	0100	C
11-23-73	0130	B
11-27-73	0730	A
11-27-73	0900	C
12-15-73	0230	A
12-22-73	0300	A
12-29-73	0600	C
12-30-73	0630	B

time increases as the proportion of spurious pulses increases, it is urged that care be taken to ensure a radio-quiet spacecraft.

(5). Sampling Techniques

A time window of duration W_t is opened at some time t_1. At the instant the window is opened an accumulation of oscillator pulses is begun. The accumulation ceases upon reception of the first Jovian burst or pulse at some time $(t_1 + \Delta t_{\beta 1})$, where $\Delta t_{\beta 1} \leq W_t$. Section IV-9 discusses the triggering electronics. The accumulator total, which is a measure of $\Delta t_{\beta 1}$, is telemetered to earth. The uncertainty with which $\Delta t_{\beta 1}$ can be measured is inversely proportional to the oscillator frequency (f_o). The pulse ranging experiment error analysis in Section IV-2 indicates that a 0.1 msec error in Δt_β is acceptable, which implies an oscillator frequency of 10 KHz. A higher frequency would allow better measurement of the pulse arrival time, but would increase the telemetry rates. Therefore, an oscillator frequency (f_o) of 10 KHz is chosen.

At time $(t_1 + T)$, where $T > W_t$, the window is opened again and the measurement procedure repeated yielding a burst time, $t_1 + T + \Delta t_{\beta_2}$. The n^{th} measured value is therefore $(t_1 + (n-1)T + \Delta t_{\beta_n})$.

The elapsed time between samples (T) is determined by the telemetry bit rate; $T \simeq 0.187$ sec at a bit rate of 512 BPS and 0.375 sec at 256 BPS.

The probability of receiving a Jovian pulse within the window width (W_t) is dependent on both the window width and the Jovian pulse or burst rate (R_{jp}). It should be noted that not every sampling window will contain a Jovian pulse or burst rise.

The accumulator which is measuring Δt_β must be shut off upon reception of the first Jovian pulse or burst. The pulse, having a rise time on the order of 10 microseconds, can be differentiated to select against slower-rising noise components. A triggering pulse will therefore be available within 10 microseconds of the arrival of a given isolated pulse.

The bursts, which are composed of noise and pulses, present opportunities to trigger on the leading edge of the burst or on one of the pulses. The noise component of the bursts normally rises above a 3 RMS background threshhold within 0.8 msec and often continues to

increase in amplitude for 3 or 4 milliseconds. The time of crossing a predetermined amplitude threshhold may therefore be determined to an accuracy of 0.1 msec.

The data resulting from this sampling scheme will be used on the ground to reconstruct a sequence of Jovian pulse or burst arrival times. This data sequence will be cross-correlated with Jovian data received directly on the earth. The value for (t_1) must be provided either by a spacecraft clock or by initiating the sampling sequence at a known time by ground command. Time must be known to an accuracy of 0.1 msec or better.

A sample interval (T) of 0.25 sec has been selected as a compromise between the 256 and 512 BPS sample intervals. There will be four sampling windows per second, with each window having a width (W_t) of 50 msec. The value of Δt_β for each window is obtained by counting the number of 10 KHz oscillator pulses which occur before the arrival of the first Jovian burst or pulse. The count for each window, which may reach a maximum value of 500, will be telemetered by a 9 bit word. The probability of telemetering exactly 1, 2, 3 or 4 rise times per second using this sampling technique is plotted in Figure IV-18 vs. Jovian burst or pulse rate. It has been assumed that the bursts and pulses both fit a Poisson distribution. The probability of telemetering at least 1, 2, 3 or 4 rise times per second vs. burst or pulse rate is plotted in Figure IV-19.

(6). Location of Solar Burst Sources

The period from launch until near Jupiter encounter offers substantial opportunity for low frequency solar radio astronomy. With launch set for 1972, the solar cycle will be well down from maximum, but probably not far from the activity level which existed when OGO-III was launched. It is reasonable to expect about ten very strong bursts and many weaker ones per month.

The wide range of available frequencies permits study of a substantial volume of the corona. The University of Michigan is developing an extensive background of knowledge on low frequency solar bursts. The extension of this analysis to the period of solar minimum is in itself justification for performing solar radio astronomy on the asteroid/Jupiter probe. An idealized orbit for the probe is shown in

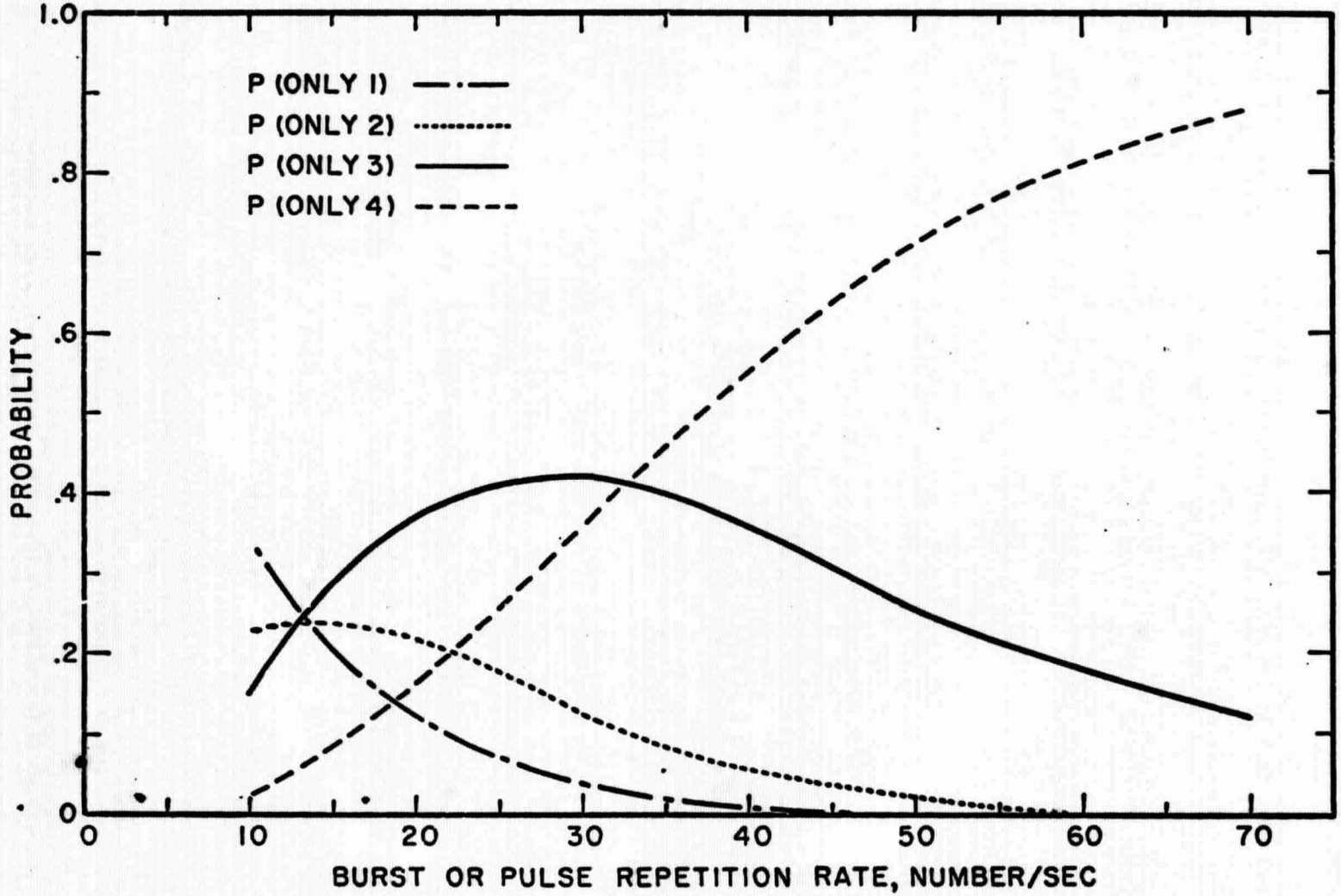

Figure IV-13. The probability of telemetering exactly 1, 2, 3, 4 events per second.

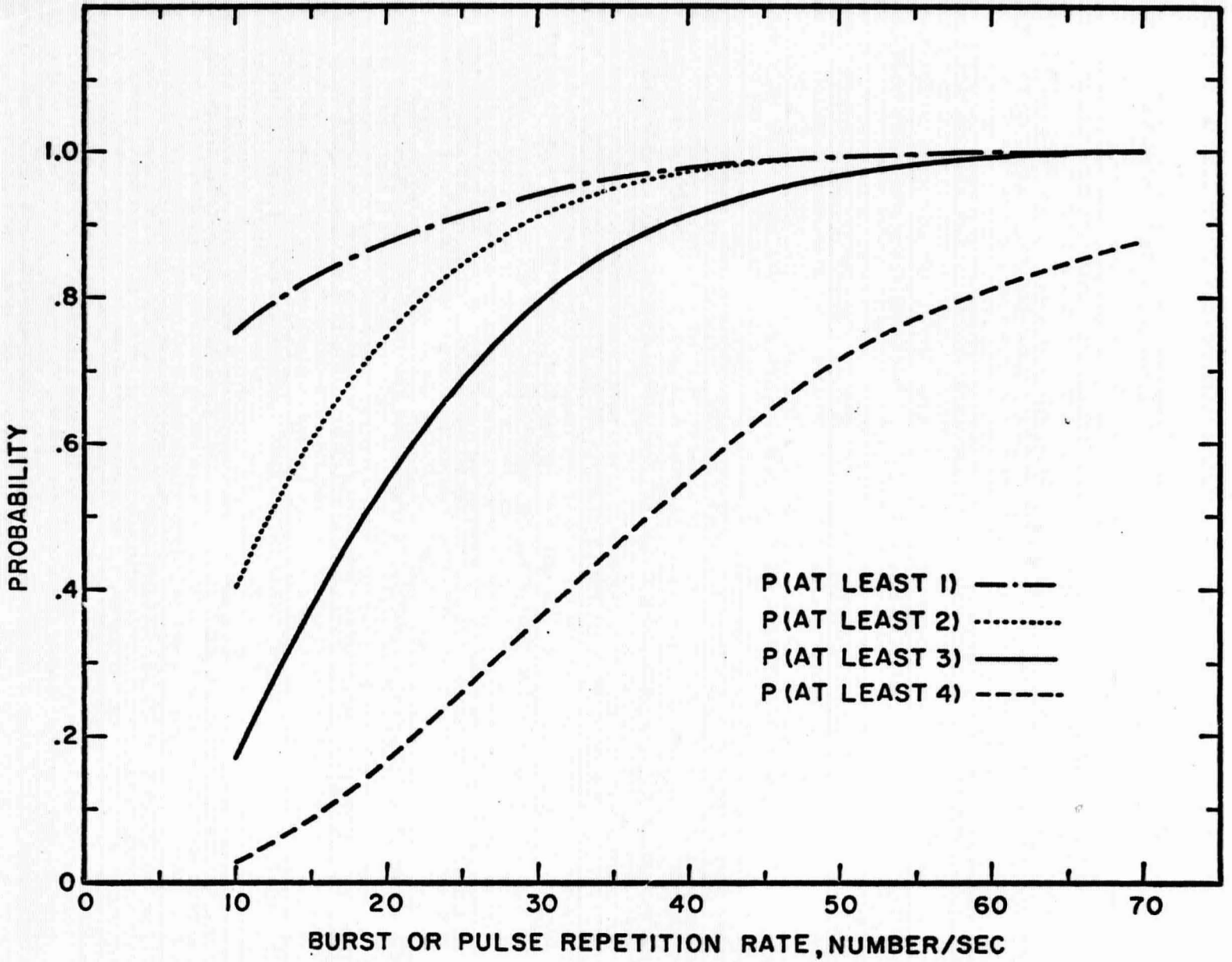

Figure IV-19. The probability of telemetering at least 1, 2, 3, or 4 events per second.

Figure IV-12. It is anticipated that most of the solar research will be carried out during the period from launch to point 5 on the path.

Opportunity for specifying more accurately the run of electron density in the outer corona (past $4R_\odot$) will be provided if either OGO-V or IMP-I is operating during the period when the asteroid/ Jupiter probe is used for solar research. The method is outlined in Figure IV-20. In this sketch, which is not to scale, a stream of high velocity electrons propagates outward from the sun in direction 1. At the dotted circle, plasma oscillations and subsequent electromagnetic radiation at the local plasma frequency take place. From the position of the burst, the angles φ_1 and φ_2 to the two spacecraft are determined. Measurement is made in the clockwise direction, with the direction of the solar center defined as $\varphi = 0°$. If the condition $90° < \varphi_i < 270°$ holds, the burst will be detected by the spacecraft in question. For $270° < \varphi_i < 90°$, the radiation will be absorbed by the solar atmosphere. For the geometry pictured, the following situations occur:

Direction	Asteroid/Jupiter Probe	OGO-V/IMP-I
1	Detection	Detection
2	Detection	Non-Detection
3	Non-Detection	Non-Detection
4	Non-Detection	Detection

The direction of the burst can be specified in several ways. The simplest is to identify the associated flaring region and assume radial motion of the particles. Second, if the High Altitude Observatory coronagraph for the Apollo Telescope Mount is aloft at the time, coronal streamer direction will be well known. Also, the time lag between burst detection at the OGO-V/IMP-I spacecraft and the Jupiter probe can provide direction information. The geometrical restrictions placed on detection then establish a height in the corona for the origin of the burst. If the two spacecraft are on opposite sides of the sun, joint burst detection will seldom or never occur. In exchange, however, the detection of low frequency solar bursts over the total range of solar longitudes is possible.

The joint burst observation experiment can also be performed at frequencies above ionospheric cut-off by combining asteroid/Jupiter probe observations with ground station observations. This technique

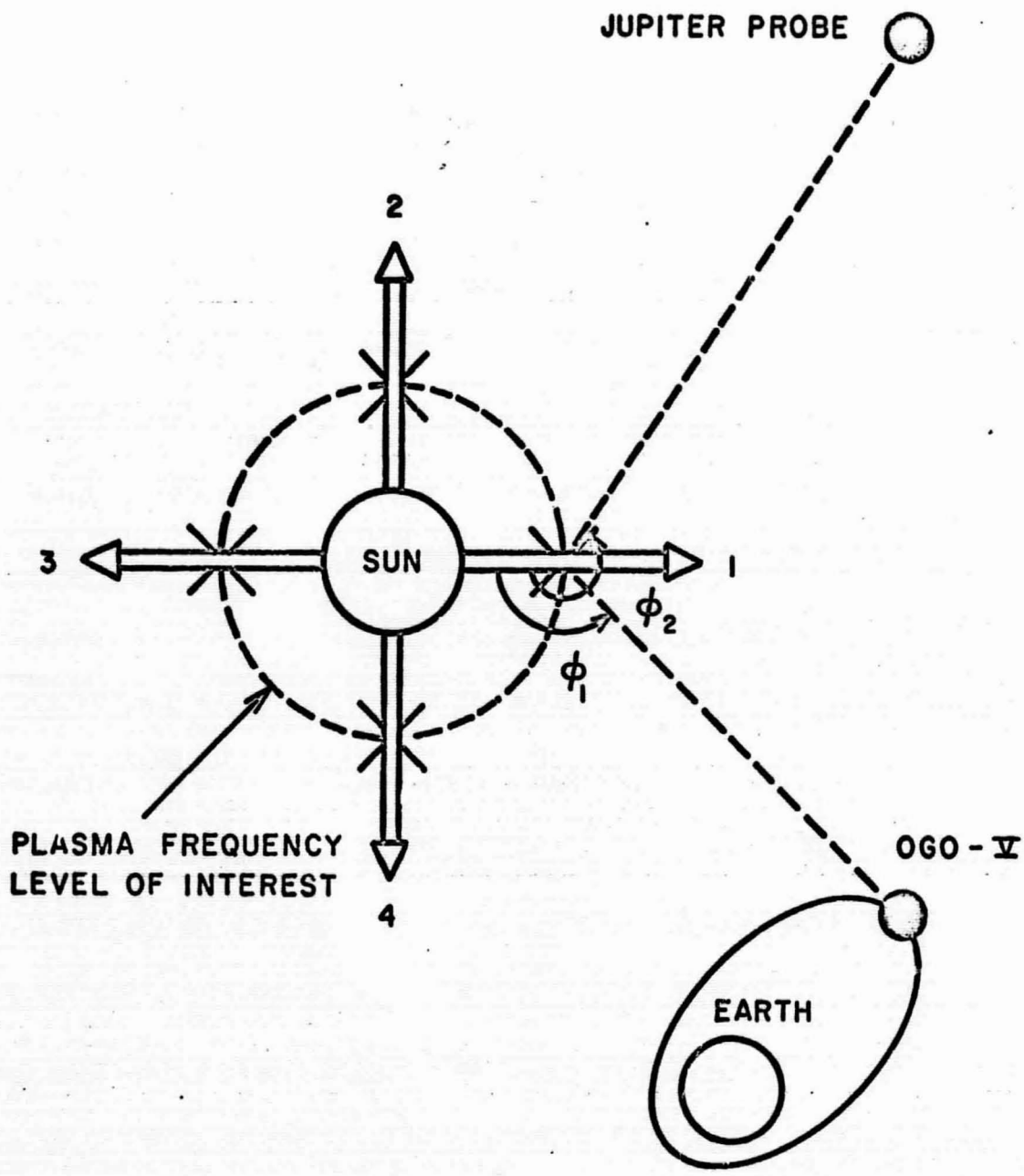

Figure IV-20. Solar burst geometry.

is of course the analog of the Jupiter pulse-ranging experiment. It will provide information on sources somewhat deeper in the corona, where the electron density profile is much better known than it is for the altitudes explored by the preceding purely space techniques. The consequent link-up will strengthen confidence in the interpretation of the overall experiment.

3. JUPITER SOURCE SIZE MEASUREMENTS

The S-source location procedure described in Section IV-2 requires that the elapsed time ($T_1 - T_2$) between the reception of an S burst or a P pulse at the spacecraft and at the earth be measured. $T_1 - T_2$ is determined by cross-correlating the sequence of pulse arrival times at the earth with that at the spacecraft. The width of the correlation peak will depend on the position measurement accuracy. This width can be thought of as a line width characteristic of the measuring system. However, further correlation peak broadening will occur if the source is larger than the systematic error in much the same manner that the fringe visibility of a phase sensitive interferometer is decreased when the source size becomes appreciably larger than the lobe width.

The ranging experiment may be thought of as an amplitude-sensitive interferometer operating at a frequency of 10 KHz. With the 0.7 A. U. effective baseline at 460 days past launch one will resolve sources having diameters as small as 3000 km, about 2% of Jupiter's disc diameter.

4. SOURCE MOTION EXPERIMENTS

(1). Jupiter Sources

Gross, relatively long-term source motions can of course be derived directly from the basic pulse-ranging experiment. However, the simple modification described below will allow one to detect and measure very rapid motions, if, for example, the source were to cascade down a magnetic field line as it is radiating in conformity with several leading models of the radiation mechanism.

Computerized techniques will be used to calculate the cross correlation functions for the pulse-ranging experiment. Before correlation peak widths are used for source size determinations, a set of velocity functions will be artificially imposed on the source by the computer,

yielding a slightly different sequence of times than was telemetered from the spacecraft. The velocity function which gives the sharpest cross correlation peak will represent the actual velocity of the source.

(2). Solar Sources

Section IV-2 describes several procedures useful in determining solar source positions. Since solar storm bursts, Type III bursts, and possibly the fine structure of other types provide time references analogous to the Jovian pulses, although on a coarser time scale, a similar pulse-ranging technique can be employed on the sun. This can be done utilizing the asteroid/Jupiter probe and a ground station or the probe and a second spacecraft which may be in earth orbit at the time. The latter would be considerably more interesting because it will yield information on the poorly known outer corona.

If the earth-orbital spacecraft involves one of the Michigan (or similar) experiments based on a swept-frequency radiometer, source position can be defined as a function of frequency over the entire band, providing the information necessary for deriving a coronal model. While the relatively slow rise time of solar bursts (typically of the order of seconds for Type III) limits pulse-ranging precision to about 0.01 A. U., the requirement for solar source positions is far less stringent than in the case of Jupiter, and the results will be of considerable interest.

5. SPECTRUM MEASUREMENTS

(1). Low Frequency Jupiter Emission

Ground-based measurements of Jupiter's decametric radio emission indicate that a substantial portion of the radio energy emitted by the planet lies at frequencies below 5 MHz, the lowest frequency observable from the ground. To examine this low frequency emission and to tie it in with neighboring emission at slightly higher frequencies, two swept-frequency receivers will be used, one operating an octave above the other.

1. Dynamic Range of the Receivers

Carr has reported Jovian 20 MHz flux levels from about S avg = 3×10^{-23} wm^{-2} Hz^{-1} to S peak = 3×10^{-20} wm^{-2} Hz^{-1}. Use of these data is conservative, since the flux levels rise rapidly (as fast as λ^8) as

one goes to lower frequencies. S min is determined by the receiver and sky brightness temperature. For the source location experiment, the post-detection time constant (τ) is 10^{-4} sec and the bandwidth (BW) is 100 KHz. At 20 MHz the sky brightness temperature is taken as 10^5 °K. The receiver temperature is assumed to be 10^4 °K. With this information one computes the detectability levels considering the system as a total power radiometer. The minimum detectable temperature turns out to be $\Delta T_{min} = 3.5 \times 10^3$ °K for the flux measurement experiment and $\Delta T_{min} = 3.5 \times 10^4$ °K for the source location experiment. To account for the enhancement of signal strength due to proximity, the r^{-2} law is assumed to hold all the way to the planet.

To express flux densities in antenna temperature T_A, the aerial is assumed to be a $\lambda/2$ dipole whose gain over an isotropic radiator is 1.64.

$$T_A = \frac{S \lambda^2}{2k \, 4\pi} G$$

Where:

G = Antenna gain = 1.64

k = Boltzman constant

λ = Wavelength = 15 m

Then:

$$T_A = 10.5 \times 10^{23} \times S \; [°K]$$

The antenna temperature produced by the average and average-peak flux densities at launch would be

(T_A) avg = 52°K

(T_A) peak = 5.2×10^4 °K

The projected Jupiter, sky, and receiver noise levels respectively are shown in Figures IV-21 and IV-22 for the ranging and flux measurement receivers. They are referred to the sky brightness temperature as zero level for the db scale. The abscissa is given in two scales: time of flight in days and distance from the spacecraft to Jupiter in A. U.

The dynamic range of the receiver is 80 db above the sky noise temperature. Both figures show that the "peak" level is always above the detectability level in both experiments. It should be noted that Carr's "peak" level is actually the mean of the stronger L-bursts received during an observing interval; it is encouraging that the stronger S bursts appear to exceed the L-burst peaks by a considerable margin.

Figure IV-21 Projected Jupiter, Sky and Receiver Noise Levels for the Pulse Ranging Experiment

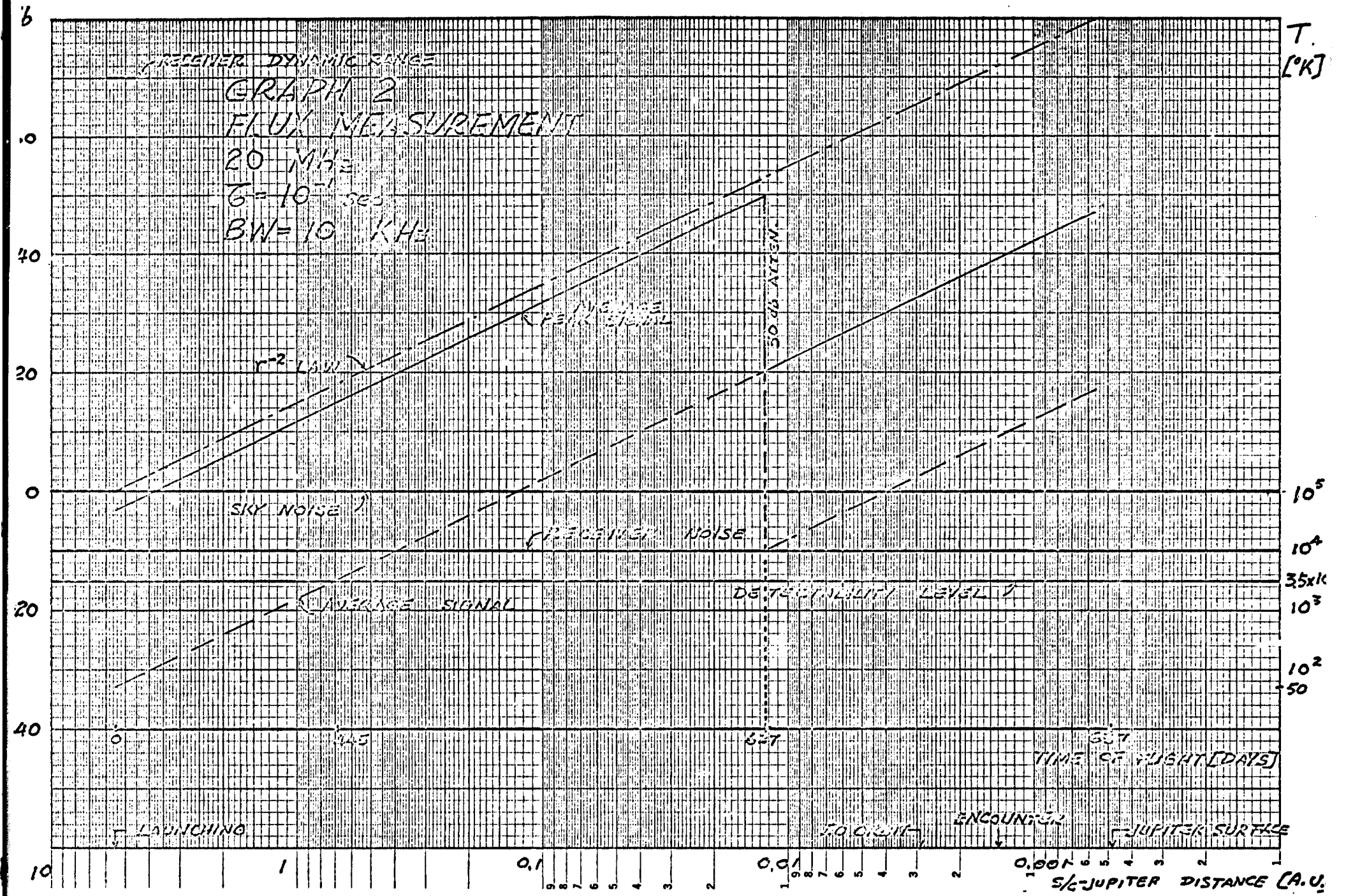

Figure IV-22 Projected Jupiter, Sky and Receiver Noise Levels for the Flux Measurement Receivers

Figure IV-22 shows an added 30 db of attenuation in the flux measurement receiver after approximately 627 days of flight. This will keep the signal between 20 and 30 db below saturation, in case the increase in level is larger than that predicted by the r^{-2} law, which could be the case when the spacecraft is immersed in the source. An even safer 40 db pad will be used in the actual experiment package.

2. Frequency Range

The L. O. frequency of each receiver will be determined by the frequency synthesizing network described in Section IV-9. Since the bandwidths of the swept receivers are 100 KHz so that they can be used to back up the pulse ranging receiver, 10 KHz predetection filters are inserted when they are being used for flux measurements. Each receiver frequency will be changed in eight logarithmic steps across the range 0.1 MHz to 21 MHz. Both receivers will operate simultaneously, one an octave above the other. Their predetection time constants will be 0.1 sec. The flux of each receiver, integrated over 0.1 second, will be digitized into a six-bit telemetry word for transmission once each main frame of the spacecraft commutator when the experiment is operating in the swept frequency mode. A special variable format mode will be available so that the sweep range can be reduced to study a particularly interesting portion of the spectrum in much greater detail.

(2). 60 MHz Jovian Radiation

The receiver characteristics are

τ = 0.1 sec

BW = 100 KHz

At this frequency the sky noise temperature is taken as 5×10^3 °K, which gives

$$\Delta T_{min} = 150°K$$

Observations by Carr using one leg of the original Mills Cross in 1964 put an upper limit of 4×10^{-25} wm^{-2} Hz^{-1} on Jupiter's 85.5 MHz radiation. This is the starting point for the curve shown in Figure IV-23 and labeled "upper bound of minimum signal level".

The 60 MHz receiver will be turned on after 622 days, when the detectability level is reached. About 10 days before encounter the power to the receiver begins to exceed the level it would reach if the 1000-foot dish at the Arecibo Ionospheric Observatory were used. If any of the 60 MHz signals possess the bursty nature of the decametric radiation, this will

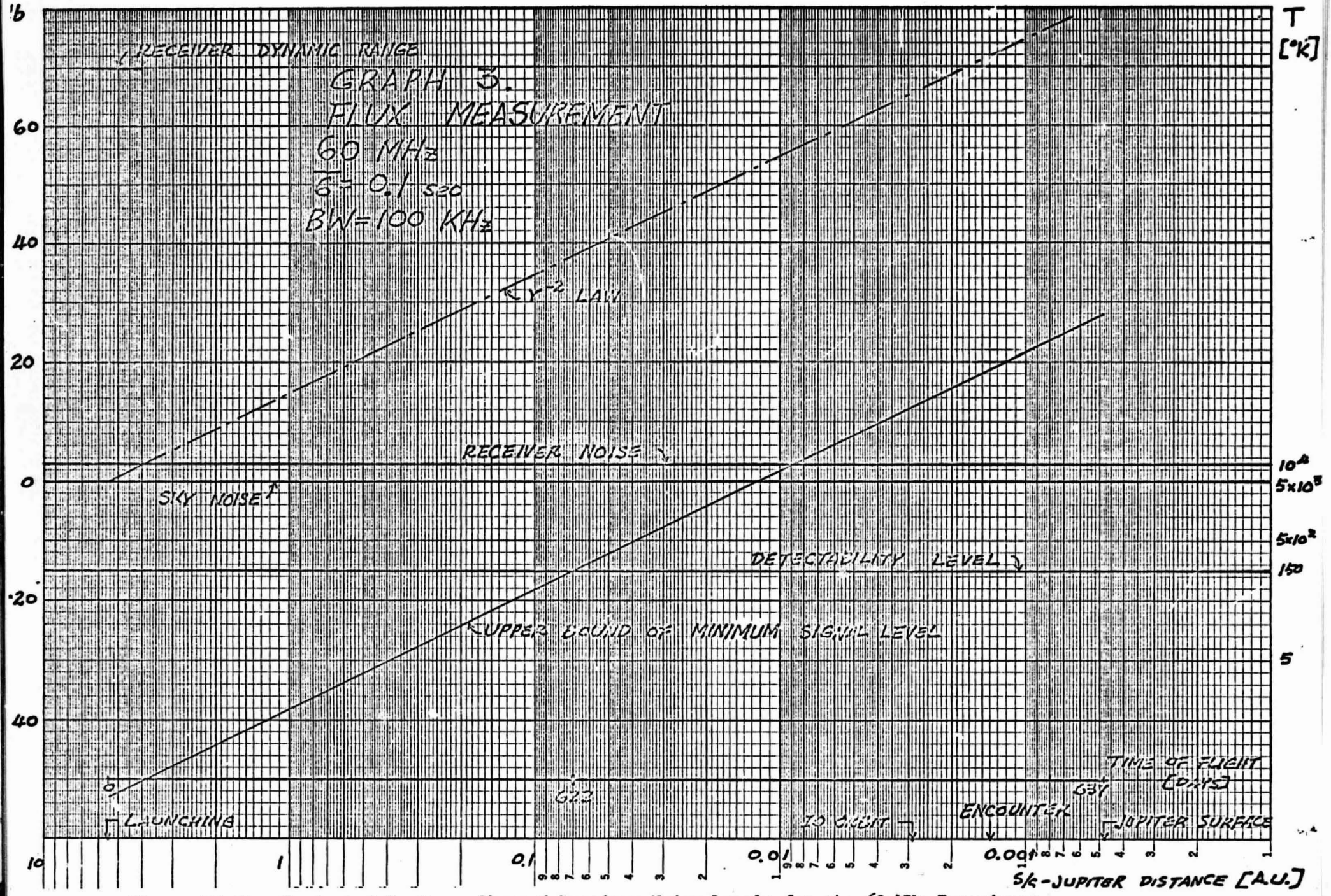

Figure IV-23 Projected Jupiter, Sky and Receiver Noise Levels for the 60 Mlz Experiment

be revealed by the burst characteristic circuitry.

(3). Solar Burst Spectra

Solar burst data will be received during the cruise mode of the mission as a by-product of the Jupiter spectral monitoring program. No additional instrumentation, telemetry, or modes of operation will be required.

6. BURST CHARACTERISTIC MEASUREMENTS

The burst characteristics unit is designed to provide information on the structure of both Jovian S- and L-type activity.

In the S-burst characteristics mode, the unit will count the number of bursts or pulses exceeding a given amplitude threshhold in a specified time interval. It will also produce a count proportional to the total time the signal spends above this threshhold in the same interval.

In the L-burst characteristic mode, the radiometer output will be put through suitable parallel low- and high-pass filters. The ratio of the filter outputs provides a direct measure of the L-burst scintillation or modulation index.

The spacecraft burst characteristic data, when compared with data taken on the earth, will indicate the true temporal nature of the sources as well as the effect of the interplanetary medium on the signals.

7. ANTENNA IMPEDANCE SCIENCE

(1). Introduction

A primary purpose of the antenna impedance measurement circuit is to provide values of antenna reactance and resistance for correcting the observed antenna temperatures. However, there are important by-products. The data can be used to derive electron densities and density perturbations in the interplanetary medium and in the vicinity of Jupiter. If measurements are made in the ionosphere and in interplanetary space, the effects on the antenna resistance of electron collision losses can be assessed experimentally. Other uses would be to supplement data from other experiments in regions such as the Jovian magnetosheath and the interplanetary-interstellar boundary, if it is encountered. The discussions which follow are oriented primarily towards these by-products.

(2). Earth Parking Orbit

If the antennas are motor driven retractable ones, a useful purpose can be served by temporarily deploying them for calibration purposes while Pioneer is in an earth parking orbit.

One of the problems with monopole or dipole antenna systems on this type of spacecraft is knowing the radiation resistance accurately. This question arises because the antenna does not look like a simple dipole, nor like a monopole over a perfect ground plane. It is therefore difficult to predict theoretically the complex impedance in free space, or anywhere else in a magneto-ionic medium. If the antennas could be deployed while the spacecraft is in an earth parking orbit, and if the orbit were high enough to put the antenna in region 1 of the $X\text{-}Y^2$ diagram (Figure IV-24) then measurements of the complex impedance, especially R_A, could be made and compared with measurements taken during the interplanetary portion of the flight.

Measurements in the two regions should provide information on electron collision loss contributions to the measured antenna resistance. During the interplanetary portion of the flight, the antenna will be in a region of very low electron density, very low magnetic field, and very low electron collision frequency; in other words, it will be essentially in free space. Theoretical antenna resistances in free space for a POGO 60-foot antenna are between 8 and 16 ohms. Measurements

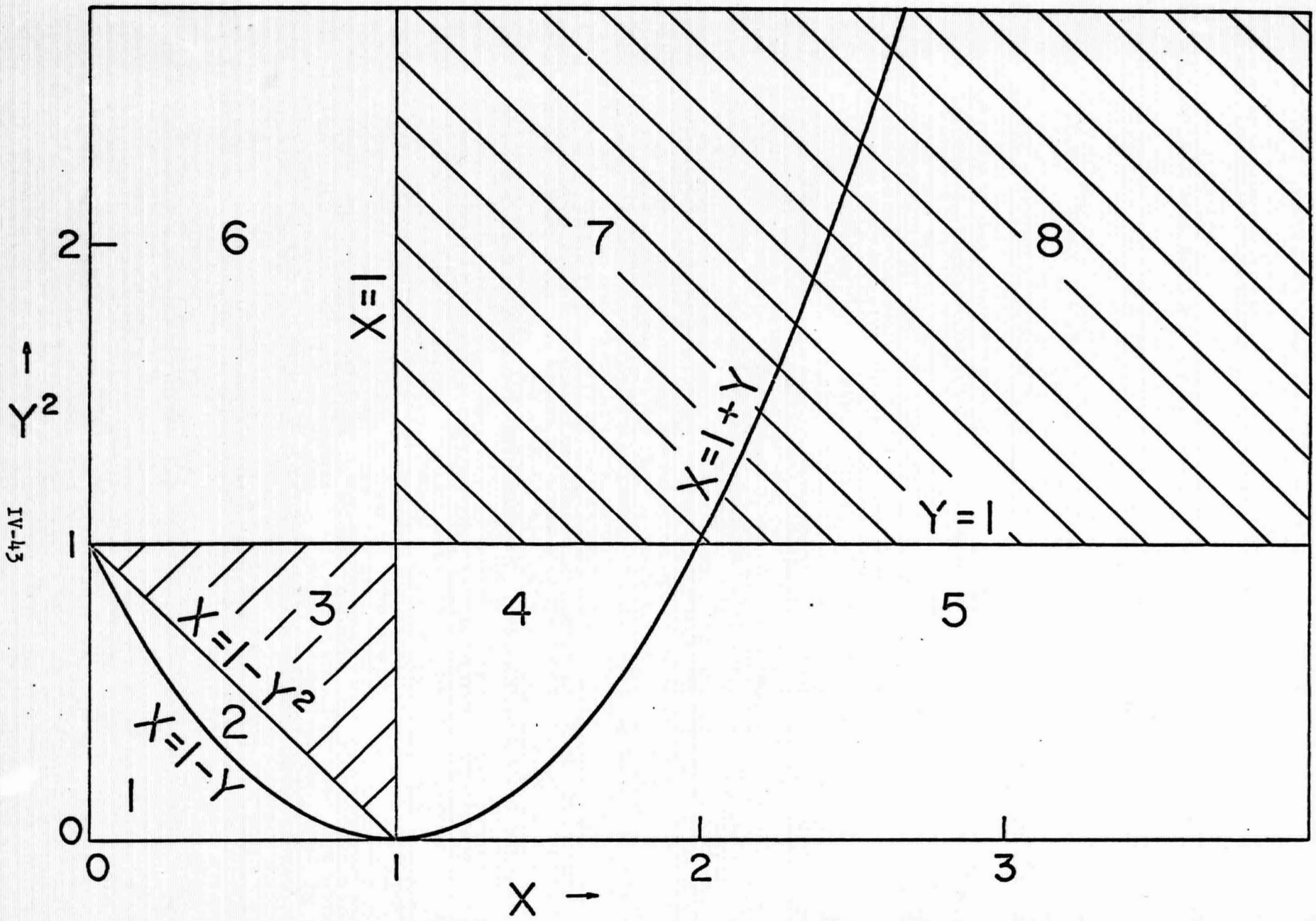

Figure IV - 24. Magnetoionic plasma regions in the X-Y^2 plane. Ionospheric noise is associated with regions 3, 7 and 8. The extraordinary wave disappears on crossing from region 1 to region 2. $Y = f_g / f$, $X = f_p^2 / f^2$, f_g = gyro frequency and f_p = plasma frequency.

on OGO-II and OGO-IV yield R_A values in the range of 110 ohms. Prof. H. Weil has recently calculated R_A in the upper f_2 region using Balmain's theory; and after inserting the electron collision frequency term has obtained an antenna loss term of 80 ohms due to collisions alone.

(3) Interplanetary Flight

Table IV-2 shows probabi values of interplanetary electron densities and magnetic field with associated plasma and gyro frequencies. The table includes ambient ionized interplanetary gas, solar wind particles and magnetic field. It is obvious from the table that for frequencies on the order of 30 KHz or greater, $Y^2 = \left(\frac{f_g}{f}\right)^2 \leq .01$, and we need be concerned only with the electron densities and plasma frequencies. For all practical purposes we will be along the abscissa of the X-Y^2 diagram.

Several types of measurements could be conducted with an antenna impedance bridge using these properties as guidelines. They include: (1) a high-frequency bridge, (2) a low-frequency bridge, (3) a multiple low-frequency plasma-frequency indicator. After careful evaluation, based on extensive experience, the second of these alternatives was selected for the Pioneer F/G experiment because of its superior rejection of spacecraft RFI as well as Jovian environmental noise. A further advantage of this system is the sensitivity to electron density changes in the various regions. A multiple-frequency impedance probe will be built at frequencies 26, 104, and 416 KHz. This will be used to detect the plasma density where the operating frequency equals the plasma frequency and to monitor solar wind fluctuations. It would be similar to a POGO sine/cosine phase-detector system. When the magnetic field is negligible, as it is in this situation, the antenna reactance will change from capacitive to inductive on going from $X < 1$ to $X > 1$.[1] This reactance reversal is easily detectable and provides a very clear indication of the electron density. More detailed study of the impedance will reveal more detail of the density distribution. Strong effects also show up on the resistive component of impedance in this essentially collisionless plasma, when the frequency is slightly above the plasma frequency.

---

[1] "Ionospheric Diagnostics Using Resonances of an Electric Dipole," W.E. Blair, Radio Science, V.3, N.2 (Feb., 1968).

TABLE IV-2. INTERPLANETARY MAGNETO-IONIC PROPERTIES

Quiet Sun Condition

$N_e = 6$ cm^{-3}	$f_p = 22$ KHz
B = 1 gamma (10^{-5} gauss)	$f_g = 28.4$ Hz

Disturbed Sun Condition

$N_e = 60 \rightarrow 600$ cm^{-3}	$f_p = 70$ KHz $\rightarrow$ 220 KHz
B = 10 $\rightarrow$ 100 gamma	$f_g = 284 \rightarrow 2840$ Hz

(4) Jupiter Encounter

By "encounter" is meant an approach distance on the order of Jupiter's magnetopause, i.e., :~ 50 Jovian radii (R_j). This is the region of significantly increasing magnetic field intensity due to Jupiter's "dipole" field. Electron density increases at this distance are probably not too significant, except perhaps in the magnetosheath. However, at distances below 10 R_j it might be reasonable to look for N_e changes due to a Jovian ionosphere, although in theory the electron density should not increase significantly until ~ 1 R_j. This latter distance probably will not be reached deliberately. It is well to take the cautious view, however, and to look for an ionosphere farther out. For approaches as close as 5 r_j above the surface (near the orbit of Io), the expected upper limits on plasma and gyro frequencies are 50 KHz and 300 KHz, respectively. When the gyro frequency is not negligible the tell-tale reactance sign change occurs at the upper hybrid frequency, $f_{UH}^2 = f_p^2 + f_g^2$; i.e., at $x = 1 - y^2$ and the radiation resistance rapid variation occurs for frequencies slightly above the upper hybrid frequency.

(5) Data Rate

If the antennas were deployed while in an earth parking orbit, it would be desirable to take a data sample every second or so. A faster rate would, however, be desirable. A slower rate would have to be considered on the basis of the eccentricity of the orbit and the

rate of change of the X and Y parameters.

During interplanetary flight a low data rate could be used to return all of the data. It would be necessary to read the spacecraft clock in the same commutator cycle.

During the encounter with Jupiter, the average data rate can still be quite low because the grazing encounter should result in slow electron density changes and slow magnetic field intensity changes.

8. Polarization Measurements.

Polarization measurements will be performed at several harmonically related frequencies within the range 0.1 MHz to 21 MHz. An orthogonal pair of antennas will be synthesized from the three monopoles, as described in Section IV-9. The outputs of these antennas are fed through appropriate phasing networks to produce right- and left-hand circular components which are in turn fed to two receivers. The telemetered receiver outputs provide an accurate measure of the polarization sense and the apparent axial ratio of the received Jovian bursts. However, the orientation of the polarization ellipse cannot be measured for bursts having durations which are short compared with the spacecraft spin rate of 1 revolution per 12 seconds.

If the quasi-continuum radiation hypothesized by Douglas is in fact present, then information concerning the orientation of the polarization ellipse may be obtained. If the pulse characteristic studies suggest that the bursts have indeed become long enough as the spacecraft approaches Jupiter, an operational mode change will connect a single monopole to one of the receivers. As the spacecraft rotates, the polarization ellipse will be traced out and its orientation in space determined. This measurement must rely on the assumption that if such a quasi-continuum exists its polarization state will remain essentially static throughout the measurement period of some 12 seconds. Axial ratio and the sense of polarization will be measured as in the preceding paragraph. Near encounter the directivity of the antenna itself and cyclic variation of the polarization parameters as the spacecraft rotates may provide limited information on the directions of the Jovian sources. However, the immersion of the spacecraft in the Jovian magnetosphere, including propagation anomalies, and local generation of

trapped radio noise, as well as the various Jovian radio-frequency beaming phenomena, will probably render interpretation of such direction-finding results at best ambiguous and at worst hopeless. Particularly difficult would be the relation of such results to the earth-based observations. It is for these reasons that the pulse-ranging approach during the cruise mode was selected as having much enhanced chances of success in the crucial matter of source location.

VI. RESULTS EXPECTED

1. SOURCE POSITION MEASUREMENTS

The pulse-ranging data are derived from the times of arrival of sharp S-type bursts or P-type pulses at the spacecraft. However, S- and P-type radiation occur only when Io and Jupiter are related in special geometries.

Shortly after launch, calibration pulses will be fed into the pulse-ranging receiver. The detected trains of pulses will be compared with the calibration pulses to check for the presence of RFI pulses. During the first fifty days the pulse-ranging receiver will be turned on during times when no Io-related emission is predicted, to measure background pulse rates. There should be few detectable pulses during these times, hence the telemetered data should include 512 clock counts each time the pulse-sampling window is opened. Anything other than 512 counts indicates that a pulse occurred. From 50 to 200 days the source position parameters R and Z will be determined to an accuracy of about 1000 km. During this period the ranging experiment will be turned on when Io-related activity is predicted. The number of data counts per telemetry word should be less than the full 512 for as many as 20 to 30 words per second. If the telemetry bit rate is higher, the number of partially filled data words will increase. From about 280 to 360 days the number of completely filled telemetry words will increase, since most of the Jupiter radiation will be absorbed in the solar corona. After 400 days, up until encounter, the ranging accuracy will be about 300 km, and hence the ranging receiver will again be activated during each Io-related noise storm. However, during this time there should be more registered pulses, i.e. more data words having less than 512 counts. As the spacecraft approaches encounter the detection threshhold may have to be increased to accommodate the higher signal levels. However, even though the number of registered pulses is high, the calculated cross-correlation function may decrease because the earth and the spacecraft may not lie in the same Jovian radiation beam (this will actually provide information on the beam characteristics).

Since the L-type bursts cannot be localized with sufficient accuracy with the pulse-ranging technique an attempt will be made at encounter to use amplitude modulation created by spacecraft spin in the output of the flux measuring receivers. If the L sources become quasi-continuous, as predicted by Douglas, cyclic variations may occur in the flux receiver outputs due to the spinning monopole antenna patterns. If the orientation of the spacecraft as a function of time is known, an effort can be made to correlate these variations with at least the virtual direction of the source(s). However, attention has been called in another section to the ambiguities and difficulties that may characterize this method of source location.

2. JUPITER SOURCE SIZE MEASUREMENTS

Source size measurements will be possible only for the S- and P-type radiation. The size determination at a given time depends on the width of the peak computed by cross correlating the ranging data and the earth-based data at that time. Part 1 in this section describes the variation of data rate with time from launch.

Early in the flight, when high data rates are available, a reliable cross-correlation function will be obtained from about 5 to 10 seconds of data if spurious noise is at a reasonable level. The width of the peak will be due entirely to the measurement error early in the flight, unless the source is wider than about 10,000 km. The source size will not be measurable at the time of sun-Jupiter conjunction, for the solar corona will shield Jupiter radiation from the spacecraft as well as producing spurious dilation effects.

Later in the flight, between 400 and 550 days, the measurement errors will be low (300 km), and the signal level will be up; hence significant correlation coefficients will again be obtainable. Any source wider than about 3000 km will increase the cross-correlation coefficient peak width.

As mentioned in part 1 of this section, although the signal levels will be high during encounter, the cross-correlation time may be quite long due to the fact that the earth and the spacecraft do not lie in the same Jovian radiation beam.

3. MOTION OF JUPITER'S SOURCES

The motion of a Jovian S- or P-type source is determined by computer analysis of the cross-correlation function mentioned in parts 1 and 2 of this section. The computer imposes different velocity functions on the source. That velocity function which best peaks the cross-correlation function represents the velocity of the source. Source velocity calculations will be made only for those times in the orbit when significant correlation coefficients can be calculated. As the spacecraft nears Jupiter, a given velocity will be more easily detectable but the correlation times may be longer due to slower telemetry rates. If the source is moving fast this computer analysis technique will prove very powerful in regaining otherwise useless data.

4. JUPITER BURST SPECTRUM

Ground-based observations indicate that the Jovian flux increases in intensity and frequency of occurrence as the observing frequency is decreased. It is anticipated that this trend may continue to on-board frequency channels somewhat below 5 MHz. However, it is reasonable to expect the spectrum to "turn over" somewhere in the ragne 0.1-5 MHz. The delineation of this inflection will be one of the theoretically interesting results of the spectral experiment.

Provision is made in the frequency synthesizer to concentrate the spectral channels for a fine analysis of interesting regions. When the general turn-over frequency is identified, it can be refined by this technique, which is set up by ground command of a preloaded alternate program in the synthesizer. If other "interesting" spectral regions are identified, the same procedure will be used.

At 627 days past launch, a 40 db pad will be inserted in all spectral channels (except 60 MHz) to protect them against overload during the encounter phase. Because of upper limits established by large earth-based antennas, the 60 MHz channel is expected to produce useful results only during the final 10 days preceding encounter.

5. BURST CHARACTERISTIC MEASUREMENTS

Section IV-9 has described instrumentation which in effect determines the ratio of peak to average power in a train of Jovian L bursts. Such a ratio can be regarded as a scintillation or modulation index in the usual sense of these terms.

If Douglas and H. Smith are correct in stating that the L bursts are formed by the interplanetary medium -- and there is considerable ground-based information to support this view -- one would expect a systematic change in the burst scintillation index as the flight progresses. Shortly after launch the index should resemble that seen at the ground. However, University of Florida data taken simultaneously over long baselines suggest that the terrestrial ionosphere imposes a slow ($\sim$ 30 sec) modulation on the envelope of the bursts. If this is correct, the latter envelope should vanish in the earliest Pioneer observations, in itself a point of major interest.

As the flight progresses, the Jovian pulse modulation index should -- according to the Douglas/Smith hypothesis -- decrease in a systematic manner. Anomalies in the rate of decrease would be of interest as indicating regions of turbulence or local condensation in the interplanetary medium. It will be of particular interest to see if there is a discontinuity in the rate as the asteroid belt is encountered and crossed.

Finally, as the spacecraft nears Jupiter, the periods of activity should appear as relatively smooth envelopes, devoid of the familiar L-burst structure. If this behavior is <u>not</u> observed, it will of course refute the hypothesis that the burst structure is interplanetary in origin and re-establish it as a genuine phenomenon of the planet itself; needless to say, this would strongly influence theories of the radiation mechanism.

The inverse situation holds for the S-bursts. Here the ground-based evidence is strong that the burst structure originates at Jupiter. Consequently, one would not expect significant changes in burst or pulse rise time, duration, or degree of modulation during the flight. The spacecraft instrumentation measures the number of crossings of a threshhold and the average time spent above that threshhold in a sampling interval; presumably these parameters should remain constant as a function of Jupiter-spacecraft distance.

6. POLARIZATION MEASUREMENTS

Polarization measurements may be conducted in two modes, as indicated in Section IV-8. The primary mode consists of measuring the output power from two radiometers. One of the radiometers measures the right-hand circular polarization component, while the other measures the left-hand circular component. Ground-based measurements indicate that Jovian burst polarization above 15 MHz is predominantly right-hand elliptical. It is anticipated that spacecraft polarization measurements in the vicinity of 15 MHz and above will therefore produce more power in the right-hand circular channel than in the left. The ratio of these two average power levels directly gives the apparent axial ratio. If the low frequency (below 10 MHz) Jovian radiation is predominantly left-hand polarized as one would predict from extrapolated ground-based measurements, the power from the left-hand circular channel will exceed that from the right.

Measurements of the polarization ellipse orientation may be performed on bursts having sufficient duration by simply connecting a single monopole to one of the radiometers. As the spacecraft spins the power from this radiometer will vary with time in such a manner as to trace out the polarization ellipse. A plot of radiometer output power vs. monopole orientation will produce the desired orientation of the polarization ellipse. (It is assumed that absolute spacecraft orientation is known as a function of time.)

During the encounter phase of the flight the antenna nulls will sweep by one or more radiating sources every 12 seconds. The nulls in the antenna pattern will produce a drop in measured power each time the null is centered on a source. The apparent direction of the sources from the spacecraft may thus be deduced if the absolute orientation of the antenna in space is known as the spacecraft rotates.

7. ANTENNA IMPEDANCE MEASUREMENTS

The frequencies of 26, 104, and 416 KHz selected for the plasma-frequency detector correspond to plasma frequency for electron number densities of approximately 8, 134, and 2144. These values are appropriate for the quiet-day interplanetary medium, coronal streamers or solar plasma clouds, and the upper ionospheres of the earth and Jupiter, respectively.

There will be a readily measurable change of sign of the reactance when $f^2 = f_p^2 + f_g^2$, i.e., at the upper hybrid frequency. In the interplanetary medium $f_g^2 << f_p^2$ and one would expect the sign change at $f \sim f_p$ on 26 KHz. There are also radical changes in the radiation resistance for frequencies slightly above the upper hybrid.

During the cruise mode, on quiet days there may be no activity even at 26 Khz. However, incidence of irregularities of solar plasma clouds or streamers will reveal their presence and morphology. Similarly, any anomolous entrainment or generation of plasma in the asteroid belt should induce counts. During the encounter phase of the mission, successive occurrences of the plasma frequency equaling the probe frequencies should be registered, as the 26, 104, and 416 KHz resonances occur with the spacecraft moving into Jupiter's magnetosphere and, possibly, upper ionosphere. The impedance measurements will enable one to deduce the distribution of the plasma density as a function of altitude, revealing whether the rise in plasma density is monotonic, or as is likely, not monotonic and locating such important features as the magnetosheath.

8. SOLAR BURST STUDIES

It is well known that solar bursts fall into various strikingly different categories, at least five of which are formally designated. Fortunately, the temporal characteristics of solar bursts are quite different from those of Jovian bursts, so that no difficulty has been experienced in distinguishing them in ground-based observations. The burst characteristic circuitry in the spacecraft will provide ample information for such indentification. A further important aid will be the ready availability of ground-based or earth-orbital data on significant solar events, which will be relatively widely spaced near sunspot minimum.

The first observations of solar radio bursts at frequencies below ionospheric cutoff were made in 1964, when the sun was in the minimum of its activity cycle. A statistically significant number of burst observations became available only in 1966, using the UM/RAO OGO-III package. OGO-V is continuing the survey, and IMP-I can be expected to contribute further data

following launch in 1970. Pioneer F/G fills in the period for the approach to solar minimum. Data over the whole solar cycle are of interest because the structure of the corona changes markedly during the cycle. The limited information on this change is largely derived from eclipse photographs, and in no case indicates the structure past about $3_{\odot}R$. Structural information can be inferred from solar radio burst measurements by a study of the variation in impulse drift rate with frequency. This parameter changes as a function of the coronal density profile.

The association of solar radio bursts with particle emission is only now becoming feasible, with the orbiting of charged-particle detection devices aboard scientific spacecraft. Correlation of on-board charged-particle observations with solar radio burst observations will place significant constraints upon solar burst emission models, and is likely to have direct application to theories of energy release in solar flares. From a theoretical standpoint the low-frequency bursts may be appreciably more useful than higher frequency observations, since evidence indicates that the former comes from regions of the corona which are essentially free from local magnetic fields, permitting considerable simplification of the theoretical equations.

A major observational result will be the detection of a given burst on radiometer channels of successively lower frequency as the burst moves rapidly outward through the corona. Since the radiated frequency is that of the local coronal plasma, the swept record provides a picture of the radial electron density profile of the outer corona, possibly out as far as the orbit of Mercury. The linear scale of the profile will be established by the several direction- and/or range-finding procedures outlined in Section IV-2. While the observational output of these procedures was outlined there, it will be repeated here in the interest of completeness. With reference to Figure IV-20 a stream of high velocity electrons propagates outward from the sun in direction 1. At the dotted circle, plasma oscillations and subsequent EM radiation at the local plasma frequency take place. From the position of the burst the angles ϕ_1 and ϕ_2 to the two spacecraft are determined. (Measurement is made in the clockwise direction, with the direction of solar center defined as $\phi = 0°$.) If the condition $90° < \phi_i < 270°$ holds, the burst is detected by the spacecraft in question. For $270° < \phi_i < 90°$, the radiation is absorbed

by the solar atmosphere. For the geometry pictured, the following situations occur:

Direction	Pioneer F/G	OGO-V/IMP-I
1	Detection	Detection
2	Detection	Non-Detection
3	Non-Detection	Non-Detection
4	Non-Detection	Detection

The direction of the burst can be specified in several ways. The simplest is to identify the associated flaring region and assume a radial motion for the particles. Secondly, if the High Altitude Observatory coronagraph for the Apollo Telescope Mount is aloft at the time, coronal streamer direction will be well known. Also, the time lag between burst detection at the OGO-V/IMP-I spacecraft and the Pioneer F/G can provide direction information. The geometrical restrictions placed on detection then provide a height determination in the corona for the origin of the burst. The joint burst observation experiment can also be performed at higher frequencies (i.e., 60 MHz or 21 MHz) by combining Pioneer F/G observations with ground station observations, in an exact analog of the Jupiter pulse-ranging experiment.

VII. FLIGHT OPERATIONAL REQUIREMENTS

1. NASA NETWORK RANGE STATION REQUIREMENTS

(1). Telemetry Antenna Requirements

At those intervals during the flight when the pulse-ranging experiment is in operation it is desirable to have maximum telemetry rates available from the spacecraft. The pulse-ranging experiment will be in operation at predetermined times totaling approximately 150 hours during the flight. Use of a 210' ground-based receiving antenna for the telemetry will be desirable during these intervals.

(2). Timing Requirements

If a spacecraft clock of sufficient accuracy (see Section IV-2) is not available, it will be necessary to know the time of reception of pulse-ranging experiment telemetry at the ground stations to an absolute accuracy of 10 μsec. Time code groups, as well as interpolation time markers, must be provided on the telemetry data tape in such manner that the time of reception of any data bit is known to an accuracy of 10 μsec.

2. GROUND COMMUNICATIONS

(1). Radio Astronomy Site Communications

Occasional voice communication capability is desirable between the radio astronomy sites participating in the pulse-ranging experiment. There will be either two or three such sites as discussed in Section IV-9. The University of Florida has experience in providing such linkage via short wave between its sites in Florida and Chile.

(2). Data Distribution

Strong Jupiter Io-related emission frequently occurs with a seven-day periodicity. It will be desirable to know the pulse-ranging experiment data quality from a given event in order to program any necessary operational changes into the spacecraft pulse-ranging system before the next Io-related emission occurs. It is therefore desirable that pulse-ranging telemetry data be made available to the experimentors within about 4 days of reception of that data.

3. TRAJECTORY REQUIREMENTS

At the time of closest encounter the spacecraft should ideally be from 2 to 4 Jupiter radii from the surface. It is desirable for the probe to pass through Jupiter's magnetic equatorial plane at a time when the spacecraft is within the orbit of Io.